

Glassy colloidal systems

F. SCIORTINO^{†‡} and P. TARTAGLIA^{*†§}

[†]Dipartimento di Fisica, Università di Roma “La Sapienza”,
P. le A. Moro 2, I-00185, Roma, Italy

[‡]INFN/CNR Center SOFT: Complex Dynamics in Structured Systems

[§]INFN/CNR Center for Statistical Mechanics and Complexity

(Received 17 August 2005; revised 12 October 2005;
accepted in revised form 14 October 2005)

This review focuses on recent developments in the theoretical, numerical and experimental study of slow dynamics in colloidal systems, with a particular emphasis on the glass transition phenomenon. Colloidal systems appear to be particularly suited for tackling the general problem of dynamic arrest, since they show a larger flexibility compared to atomic and molecular glasses because of their size and the possibility of manipulating the physical and chemical properties of the samples. Indeed, a wealth of new effects, not easily observable in molecular liquids, have been predicted and measured in colloidal systems. The slow dynamic behavior of three classes of colloidal suspension is reviewed – hard colloids, short-range attractive colloids and soft colloidal systems – selecting the model systems among the most prominent candidates for grasping the essential features of dynamic arrest. Emphasis is on the possibility of performing a detailed comparison between experimental data and theoretical predictions based on the mode coupling theory of the glass transition. Finally, the importance of understanding the system’s kinetic arrest phase diagram, i.e. the regions in phase space where disordered arrested states can be expected, is stressed. When and how these states are kinetically stabilized with respect to the ordered lowest free energy phases is then examined in order to provide a framework for interpreting and developing new ideas in the study of new materials.

	PAGE
1. Introduction	472
2. Theoretical background	473
2.1. Mode coupling theory	473
2.2. MCT features	475
2.3. Other theoretical approaches	479
3. Hard colloids	480
3.1. Hard sphere colloids	481
3.2. Polydisperse hard spheres	485
3.3. Hard ellipsoids	487
4. Attractive colloids	490
4.1. MCT predictions	491
4.2. Experiments	494
4.3. Numerical studies	498

*Corresponding author. Email: piero.tartaglia@phys.uniroma1.it

4.4. Higher-order singularities	499
4.5. Mechanical properties	500
4.6. Remarks on attractive colloids	502
5. Soft colloids	504
5.1. Charged colloids and the Wigner glass	504
5.2. Competing interactions: cluster phases	509
5.3. Ultrasoft colloids: star polymers	515
6. Perspectives and conclusions	517
Acknowledgements	518
References	518

1. Introduction

Dynamically disordered arrested states are commonly found in soft condensed matter. Examples of this category of phenomena are the liquid–glass transition and the sol–gel and percolation transitions. As compared to molecular and atomic systems, in which dynamic arrest is associated commonly to a glass transition phenomenon, colloidal systems show a much wider range of possibilities, brought in by the wider variety of interparticle potentials, by the presence of supra molecular ordering, by the possibility of acting on the system with external fields and by their intrinsically longer time scales. In most of these cases, dynamic arrest is foreseen by a progressive slowing down of the dynamic processes, both for the tagged particle motion and for the collective rearrangements. Small changes in the external parameters bring in changes in the characteristic times, which span several orders of magnitude. Dynamics can become so slow that during the experimental observation time the system evolution is frozen in a structure which depends on the sample previous history. Despite the diversity of the arrested state, the slowing down of the dynamics which precedes dynamic arrest share common features, suggesting the idea of an underlying common explanation, or even universality, to the different manifestations of the arrest of the particles dynamics. Similarities between the slow dynamics observed in thermoreversible physical gels [1, 2], associating polymers at low concentration [3], micellar systems [4], star polymer mixtures [5], colloidal gels [6, 7], block copolymers [8] do call for a common interpretation paradigm. Recent reviews of various aspects of structural arrest in soft condensed matter systems are due, starting from the most recent one, to Cipelletti and Ramos [9], Trappe and Sandkühler [10], Dawson [11] and Poon [12].

Notwithstanding many efforts, at present there is still no comprehensive theoretical treatment of these phenomena, but only specific approaches to the various forms of structural arrest. However, the study of slow dynamics in colloidal systems appears to be particularly suited for tackling the general problem of arrest. This is due to a strong interaction between experiments, theory and simulation work and to the possibility to select common model systems, made possible by today’s ability in manipulating the physical and chemical properties of the samples. The large number of applications of this joint effort to diverse colloidal systems will hopefully bring research in this field closer to a comprehensive explanation of dynamic arrest.

The present review aims at presenting recent developments and discoveries in the slow dynamics of colloidal systems. We limit ourselves to discussing the slow

dynamics of some model systems and some physical observables that we consider to be the most prominent candidates for grasping the essential features of dynamic arrest, and which allow for a detailed comparison between the experimental data and theoretical predictions. We focus mostly on the dynamics in equilibrium close to the glass line, touching only marginally all the issues involved in the aging dynamics of the out-of-equilibrium arrested states, for which a satisfactory theoretical understanding is still lacking. For the same general reasons, we focus more on the dynamics close to a glass transition than on the slowing down observed close to gel states.

More specifically, the review is organized as follows. The starting point is an extended summary of the ideal mode coupling theory (MCT), a theory which offers detailed predictions for both self and collective dynamics and for the shape of the dynamic arrest line in the phase diagram. Recent applications of the theory to particles of (simple) non-spherical shape significantly enhance the possibility of quantitatively comparing theoretical predictions with numerical and experimental works. We then discuss recent developments in some model systems, distinguishing various types of colloids according to the interparticle interactions, starting from colloids where only a hard repulsive interaction is present. We then introduce colloids in which a short-range attractive potential is added, since they give rise to a new type of glass characterized by a rich phenomenology. The short-range attractive model systems have the potentialities to help us connect the slow dynamics in colloidal systems with the similar phenomenon observed in atomic and molecular glasses. Finally, we discuss soft colloids where long-range repulsive interactions, due e.g. to electric charges on the particles, play an important role and generate cluster phases and transition to gels. In all cases, we attempt to provide also information on the ordered crystal phases and on the possible second-order transitions, to provide a picture of the arrest process in the system phase diagram. We conclude with the perspectives and the new directions of this rich field of research.

2. Theoretical background

2.1. Mode coupling theory

The most successful approach to the glass transition in colloidal systems is the mode coupling theory, which dates back to the mid-1980s [13] and has been developed since then mainly by Götze and coworkers [14–16]. MCT has been shown to be capable to interpret in a quantitative way, to a 20% level of accuracy, experimental data close to a supercooled liquid–glass transition. The name ‘mode coupling’ was borrowed by the successful theories of dynamical critical phenomena, since in analogy with the latter the relevant variable is identified in the local density, and a non-linear (quadratic) coupling among density modes is explicitly considered in the kinetic evolution equations. In the MCT the input static quantity is the wave vector k -dependent static structure factor S_k , but contrary to critical phenomena, close to the glass transition there is no static singularity leading to a diverging correlation length and to the Ornstein–Zernike anomaly of the structure factor. The added difficulty of the theory, compared to the critical phenomena, is related to the

fact that all length scales are equally important and have to be taken into account simultaneously. MCT predicts only a kinetic singularity in the evolution equations, which leads to an ergodic to non-ergodic transition characterized by the non-vanishing of the long time limit of the density correlation functions.

The original derivation of MCT makes use of the projection operators technique of statistical mechanics [14], but other procedures have been used in order to derive the equations [17–20]. Consider N particles of mass m , in the cubic volume V , that have coordinates $\{\mathbf{r}^N\} = \{\mathbf{r}_1, \mathbf{r}_2, \dots, \mathbf{r}_N\}$. The local density is defined as

$$\rho(\mathbf{r}) = \sum_{j=1}^N \delta(\mathbf{r} - \mathbf{r}_j)$$

and gives the number density $n = \langle \rho(\mathbf{r}) \rangle$. Its spatial Fourier transform with wavevector k is

$$\rho_k = \int_V d\mathbf{r} e^{i\mathbf{k}\cdot\mathbf{r}} \rho(\mathbf{r}) = \sum_{j=1}^N e^{i\mathbf{k}\cdot\mathbf{r}_j}.$$

MCT derives equations for the normalized time-dependent density correlators of the Fourier components of the particle density deviations $\delta\rho_k(t)$

$$\Phi_k(t) \equiv \frac{\langle \delta\rho_k(t) \delta\rho_{-k}(0) \rangle}{\langle |\delta\rho_k|^2 \rangle}$$

starting only from the number density n and the structure factor $S_k = \langle |\delta\rho_k|^2 \rangle / N$.

For Newtonian dynamics, the evolution equations read

$$\frac{\partial^2}{\partial t^2} \Phi_k(t) = -\omega_k^2 \Phi_k(t) - \int_0^t dt' M_k(t-t') \frac{\partial}{\partial t'} \Phi_k(t')$$

with initial conditions $\Phi_k(0) = 1$ and $\partial\Phi_k(0)/\partial t = 0$. Here $\omega_k^2 \equiv k^2/(m\beta S_k)$ are characteristic frequencies, with $\beta = 1/(k_B T)$, where T is the temperature and k_B the Boltzmann constant. The kernels $M_k(t)$ are expressed in terms of correlators of the fluctuating forces, which in colloids include the effect of the interactions with the solvent particles. The characteristic time scale of these interactions is much shorter than the time scale of the colloidal particles dynamics, therefore they can be approximated as a friction force of the form $v_k \partial\Phi_k(t)/\partial t$, with v_k microscopic damping coefficients. Moreover, in the case of colloidal systems the propagation of the density fluctuations is controlled by the Smoluchovski equation. In this case the friction term is large compared to the inertia term $\partial^2\Phi_k(t)/\partial t^2$, which can be neglected and implies Brownian rather than Newtonian dynamics. The MCT equations for colloids are then of first rather than of second order

$$v_k \frac{\partial}{\partial t} \Phi_k(t) + \omega_k^2 \Phi_k(t) + \int_0^t dt' M_k(t-t') \frac{\partial}{\partial t'} \Phi_k(t') = 0$$

with the initial condition $\Phi_k(t) = 1$. The v_k term goes to a constant in the limit of k going to zero, differently from the k^2 behavior characteristic of Newtonian dynamics. Within MCT, all features of the short-time dynamics enter the glassy dynamics via an overall time scale t_0 only. The complete dependence of the glassy dynamics on k

and from the distance from the glass line for Newtonian and stochastic dynamics is identical, except for the choice of t_0 [21]. Therefore, according to MCT it does not matter whether glassy dynamics is analyzed in simulations for Newtonian or for stochastic dynamics. This was shown explicitly by Gleim *et al.* [22] and, more extensively by, Voigtmann *et al.* [23].

The kernels $M_k(t)$ are decomposed as the sum of a regular term $M_k^{reg}(t)$, which contains normal effects in colloids such as hydrodynamic interactions, and mode coupling contributions of the form $\omega_k^2 m_k(t)$. In the MCT calculations we report, hydrodynamic interactions are not explicitly taken into account

In the limit of quadratic nonlinearities, the memory kernel is given by

$$m_k(t) = \frac{n}{V} \sum_{k' \neq k} S_k S_{|k-k'|} S_{k'} \left| \frac{\mathbf{k} \cdot \mathbf{k}'}{k^2} c_{k'} + \frac{\mathbf{k} \cdot (\mathbf{k} - \mathbf{k}')}{k^2} c_{k-k'} \right|^2 \Phi_{|k-k'|}(t) \Phi_{k'}(t)$$

in terms of the structure factor S_k or the short-range correlation function $nc_k = 1 - S_k^{-1}$.

The glass transition predicted by MCT is obtained solving the $t \rightarrow \infty$ limit of the equations for the normalized correlators $\phi_k(t)$, the so-called non-ergodicity factor f_k

$$f_k = \lim_{t \rightarrow \infty} \Phi_k(t).$$

The equations have the form

$$\lim_{t \rightarrow \infty} m_k(t) = \frac{f_k}{1 - f_k}$$

The solution to these equations admits not only the usual trivial solution $f_k = 0$, but also solutions with $f_k \neq 0$. The value of f_k at the transition point is denoted f_k^c . In MCT language, the transition is called a type B transition when f_k grows discontinuously on entering in the non-ergodic phase, and type A transition when f_k grows continuously from zero. The non-ergodic solutions $f_k \neq 0$ depend on a number of control parameters, usually volume fraction of the colloidal particles and attraction strength. The theory accounts also for so-called higher-order singularities related to bifurcation theory (named A_3 , A_4), whose realization requires a fine tuning of the interparticle potential parameters. The A_3 bifurcation is the end point of a type B transition.

The existence of a singularity of purely kinetic origin – not related to any thermodynamic singularity, such as in the case of MCT of critical dynamics – is the most important prediction of the theory. The physical interpretation of the non-ergodicity transition is related to the well-known cage effect, the difficulty of a particle to move due to the crowd of the surrounding ones. Motion of the particle can only take place if a collective rearrangement of the particles forming the cage opens up a passage for the arrested particles.

2.2. MCT features

One of the merits of MCT is to identify the universal features of the temporal decay of density correlators in terms of asymptotic power laws of approach to the ideal glass transition. In order to properly define the asymptotic laws, it is preliminarily

necessary to define a parameter ϵ which quantifies, in terms of a control parameter x , the distance from the kinetic transition at x_c

$$\epsilon = \frac{x - x_c}{x_c}.$$

It is usually related to the fractional distance from the transition expressed in terms of volume fraction $\phi(x = \phi)$ or temperature ($x = 1/T$). A convenient way of describing the universal characteristics of the decay is to introduce its relevant time scales and the behavior of the time correlators in the various time ranges, namely:

- (i) The region of the microscopic decay related to a short-time scale t_0 of the order of the Brownian time scale in colloidal systems and of the order of the inverse phonon relaxation frequency in Newtonian systems.
- (ii) The β -relaxation region corresponding to the decay toward a plateau f_k^c and the further decay below the plateau when $\epsilon < 0$, while there is ergodicity breaking for $\epsilon > 0$. In the vicinity of the plateau MCT proposes a general expression for the density correlators of the form

$$\Phi_k(t) = f_k^c + h_k \sqrt{\epsilon} g_{\pm} \left(\frac{t}{t_{\epsilon}} \right),$$

where the subscript in g_{\pm} corresponds to the sign of ϵ , which goes under the name of factorization property, since the space and time dependencies separate, and scales with the characteristic time t_{ϵ}

$$t_{\epsilon} = t_0 |\epsilon|^{-1/(2a)},$$

which in turn scales with an exponent related to the quantity a . The non-ergodicity factor f_k^c , the critical amplitude h_k and the β -correlator g_{\pm} , are independent from ϵ . Given a particular system, g_{\pm} is a function which can be determined knowing n and the interparticle potential, which determines the structure factor S_k . The leading behavior of the function $g_{\pm}(t/t_{\epsilon})$ above or below the non-ergodicity plateau is given by the power-law in time valid for $t/t_{\epsilon} \ll 1$

$$g_{\pm}(t/t_{\epsilon}) \approx (t/t_{\epsilon})^{-a}$$

with $0 < a \leq 1/2$, while for $t/t_{\epsilon} \gg 1$ the well-known von Schweidler law is valid, with

$$g_{-}(t/t_{\epsilon}) \approx -(t/t_{\epsilon})^b$$

and $0 < b \leq 1$. It is possible to relate both exponents a (for t_{ϵ} and g_{\pm}) and b through the following relation involving the Euler Γ function

$$\frac{(\Gamma(1-a))^2}{\Gamma(1-2a)} = \frac{(\Gamma(1+b))^2}{\Gamma(1+2b)}.$$

As for the case of critical phenomena, exponents and critical laws are expected to be robust with respect to changes of system, while actual value of the kinetic transition is significantly affected by the approximations employed in MCT.

- (iii) The α -decay regime is the last stage of the decay, the cage break-up, and is characterized by a time scale τ which diverges on approaching the transition as a power law

$$\tau \approx |\epsilon|^{-\gamma} \tag{1}$$

where the exponent γ is given by

$$\gamma = \frac{1}{2a} + \frac{1}{2b}.$$

The time scale τ enters the so-called time-temperature superposition relation

$$\Phi_k(t) = F_k\left(\frac{t}{\tau}\right)$$

where $F_k(t/\tau)$ is a master function of the scaled time t/τ which allows to draw a master plot of the density correlators. A good approximation of this function is very often given by the stretched exponential function

$$\phi_k(t) = A_k e^{-(t/\tau_k)^{\beta k}}.$$

A sketch of the typical shape of the density correlators, highlighting the different time regions described by MCT, is shown in figure 1.

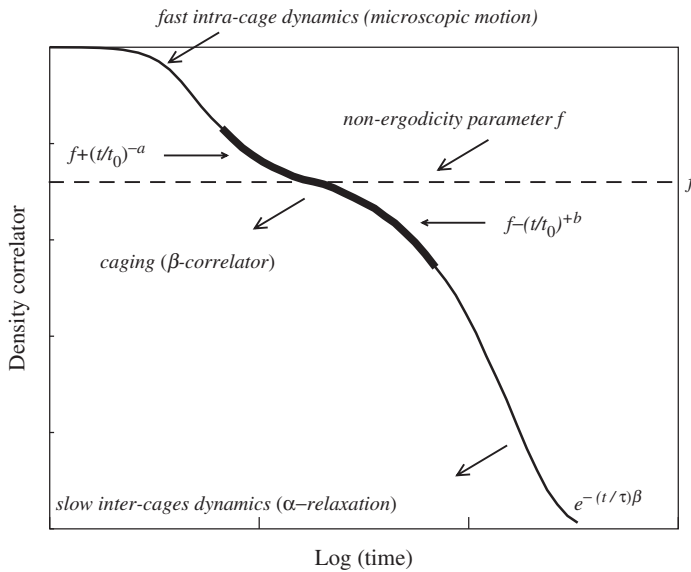


Figure 1. Sketch of the typical shape of the density correlators in the liquid, close to the glass transition. The figure highlights the different time regions in the decay of the correlations. The initial microscopic intra-cage dynamics (non-universal) is followed, according to MCT, by a time region where universal features of the caging dynamics are observed and described by the β -correlator g_- , around the non-ergodicity parameter f . The leading terms in g_- are power law functions. This region is followed, in the liquid side, by the cage-restructuring decay which can be well modeled by a stretched exponential function.

Many aspects of the predictions of the ideal MCT have been tested in detail in various systems, both experimentally and using computer simulation, with good results. More recently MCT has also shown a relevant predictive power in the important field of glassy colloidal systems dominated by attractive interparticle interactions, where a number of interesting new phenomena have been discovered and will be discussed at length in the next sections.

Many attempts have also been made to improve the ideal MCT, including the early extensions of the theory due to Götze and Sjögren to account for activated hopping processes [24]. This is obtained through a coupling to current modes, besides the density modes, which destroy the ergodic–non-ergodic transition below the mode coupling temperature. Das and coworkers [25] have derived a set of MCT-like dynamic equations, called self-consistent MCT, starting from hydrodynamics and using field theoretical techniques to handle nonlinear mode coupling terms. The non-ergodicity transition disappears with the inclusion of current correlations with density fluctuations [26]. The approach has been recently reviewed [27] and applied to binary hard spheres (HS) and Lennard-Jones systems [28], where a dependence of the dynamic transition point on the mass-ratio of the components has been observed. However, it was pointed out by Götze and Voigtmann [29] that the dependence of the mass is not consistent with the standard MCT approach.

More recently Szamel [30] has introduced an attempt to go beyond MCT, using a novel way of factorizing higher-order correlations entering the dynamic equations. The new theory applies to concentrated colloidal suspensions and predicts, like MCT, ergodicity breaking but at a volume fraction higher compared to the ideal MCT value and closer to the experimental value. Szamel also discussed difficulties of going beyond MCT both theoretically [31] and by numerical simulation [32]. Schweizer and Saltzman [33, 34] have developed a microscopic kinetic description of single-particle transient localization and activated transport in glassy colloidal fluids, which combines elements of MCT, density functional theory and activated rate theory. A Langevin equation is constructed in which the driving force contains terms favoring particle localization and the random force terms that restore ergodicity through barrier hopping. The comparison with experimental results, performed in the absence of adjustable parameters, was performed for HSs systems and limited to tagged particle properties.

Finally Wu and Cao [35] have formulated a higher-order mode coupling theory for the colloidal glass transition based on a matrix formulation for stochastic dynamics. To lowest order the theory reduces to the usual MCT, while second and third order give corrections to it. The volume fraction for the glass transition of HSs, $\phi = 0.553$, is closer to the experimental value, and the non-ergodicity factor compares favorably with experiments.

The study of the slow dynamics in colloidal systems has benefitted a lot from the possibility of a close comparison between theoretical predictions and experimental or numerical findings. The present review brings together much of the emerging experimental and numerical evidence that gives MCT increasing support. Nevertheless, we have to warn the reader that the limit of validity of MCT, especially in the most used formulation which neglects activated processes, remains controversial. Indeed, neglecting activated processes is probably a safe approximation only in the HS case and when excluded volume is the driving force for caging.

Activated processes may not be neglected when the attractive part of the interparticle potential plays a significant role in the caging process. Indeed, in the case of molecular MCT [16] (and apparently also network forming liquids [36, 37]) the ideal MCT predictions for the α -relaxation (e.g. the power-law dependence of the characteristic time, equation 1) properly describe only the first three to four orders of magnitude in the slowing down of the dynamics. Depending on the material, the location of the MCT glass line (which retains only the meaning of cross-over from a power-law growth of the α -relaxation time to a super-Arrhenius dependence) can be very different from the location of the line at which arrest is observed on an experimental time scale (the calorimetric glass transition temperature). It is unfortunate that the full form of the extended MCT, which formally includes activated processes, cannot be compared to experimental or numerical data, except in a schematic version which neglects the wavevector dependence [38–40].

2.3. Other theoretical approaches

A complete account of the theories of the glass transition is outside the scope of this review, which is limited to colloidal systems where MCT is considered to be the most appropriate and direct quantitative approach. We therefore simply make a partial list of the various theoretical approaches developed so far for understanding the slowing down of the dynamics in structural glasses.

- (i) An important contribution to the theory of glasses was given by the prototypical model of spin glasses of Sherrington and Kirkpatrick [41] and the Parisi solution of its mean field approximation [42]. This approach has clarified the physical ideas and the concepts, such as replica symmetry breaking and configurational entropy, that have opened the way to other approaches. These ideas have been transferred to the field of structural glasses in the theory of Mézard and Parisi [43, 44], based on the replica-symmetry-breaking method, which has been applied to hard [45] and soft spheres [46] with good qualitative results. They study the glass transition in the hypernetted chain (HNC) approximation by means of an effective potential, and find a transition scenario analogous to that of long-range disordered systems with one-step replica symmetry breaking.
- (ii) The potential energy landscape (PEL) approach of Stillinger and Weber [47] focuses on the statistical properties of the system in the configuration space. It is interesting to observe that the free energy expression based on Stillinger and Weber approach are conceptually similar to those derived on the basis of disordered spin models for structural relaxations [48]. The PEL approach has been useful in clarifying many aspects of the physics of glasses [49].
- (iii) A more general kinetic approach to supercooled liquids was proposed some time ago by Kawasaki [50], who introduced in the seventies the idea of non-linear coupling of hydrodynamic modes in critical dynamics. The equations derived, called dynamic density functional theory (DDFT), can be written as functional Fokker–Planck equations or as Langevin equations with multiplicative noise [51]. These equations are difficult to handle, and only some preliminary attempt has been made to solve them [52], but according to the

authors the solution has the correct equilibrium properties and should incorporate activated processes. Similar attempts have also been reported by Miyazaki and Reichman [53] using equations analogous to the ones of DDFT, derived using field theory with multiplicative noise.

- (iv) Recent studies of the glass transition have focused on the random first-order transition theory of glasses [54, 55]. This theory starts from exactly solvable mean field glass models, but extend them to include activated motions by considering entropic droplets [55]. The theory provides estimates of measurable quantities near the glass transition for a wide range of substances. In this picture, a viscous liquid or glass consists of a mosaic of frustrated domain walls separating regions of energetically less frustrated material. Each mosaic cell resembles a local minimum of the free energy, or the PEL local minimum [47].
- (v) Dynamical heterogeneities [56] are the basis of the theoretical approach of Chandler and coworkers [57, 58]. Indeed, it has been shown experimentally and by numerical simulation that, as the temperature approaches the glass transition, mobility develops spatial inhomogeneity at a mesoscopic scale. In this theory the heterogeneities are described in terms of local mobility excitations that propagate with facilitated dynamics, i.e. mobile particles facilitate the dynamics of neighboring ones, thus creating clusters of faster molecules. The facilitated dynamical models focus on the constraint on the motion of the particles, without postulating an underlying static anomaly.
- (vi) The importance of the hydrodynamic interactions in concentrated HS suspensions was stressed by Tokuyama and Oppenheim [59, 60] and applied to supercooled colloidal liquids near the glass transition [61–63]. No divergence of the relaxation times is found, although the dynamical properties of the colloids show a drastic slowing down.
- (vii) Finally, it is worth mentioning the role of some lattice models that have helped in clarifying some elementary aspect of the dynamics of the glass transition. Among these, the kinetically constrained lattice model of Kob and Andersen [64] and the model introduced by Biroli and Mézard [65] are noteworthy. Recent work in this direction by Dawson and coworkers [66–68] introduces the dynamically accessible volume as an order parameter, and identifies two distinct regimes which show slowing down of the dynamics, with a sharp threshold between them.

Unfortunately, although these theories are useful in clarifying the fundamental aspects of the glass transition, none of them provides detailed predictions for the wavevector dependence of the density correlations, and for the shape of the glass transition line in the temperature and packing fraction plane, preventing the possibility of an accurate comparison with the slow dynamics in colloidal systems. On the contrary, the comparison is possible using MCT.

3. Hard colloids

Hard colloids constitute an idealized version of a system composed by particles which experience no forces among themselves unless they are in contact.

When particles touch, they experience an infinite repulsion, preventing overlap. Thus, the pairwise additive interaction potential arises only due to the excluded volume effect. To experimentally realize the ideal hard-interaction case, it is necessary to suppress the inevitable van der Waals (short-range) attraction arising from polarizability [69]. To this aim, particles are chemically treated, for example via steric stabilization, to prevent close approach. To further reduce the effect of van der Waals interactions (and at the same time reduce turbidity) particles are often dispersed in a solvent of comparable refractive index. Steric stabilization requires the grafting of polymer chains on the surface of the colloidal particle. Similarly, a density match between solvent and colloidal particles is often implemented to minimize the effect of gravity.

3.1. Hard sphere colloids

One of the most studied model system, approaching the ideal HS case [70], is composed by poly-(methyl methacrylate) (PMMA) particles, grafted with a layer of poly-(12-hydroxy stearic acid) (PHSA) in a solvent composed by decalin and tetralin. It has been shown that the equation of state does not deviate from the one of a perfect HS system under any relevant experimental condition [70], for particle sizes larger than 50 nm in diameter and for packing fractions as large as 0.64.

The HS is a model system for studying structure and dynamics of liquids, crystals and glasses and the thermodynamic transitions between them. It is often used as reference model for evaluating properties of more sophisticated and realistic potentials [71]. The phase diagram of HS of uniform size depends only on the packing fraction ϕ . Computer simulation studies, in the late-1950s [72], provided evidence that the HS fluid, despite the absence of any attractive part in the potential, crystallized when $\phi > 0.49$. Up to $\phi = 0.545$, the crystal phase coexists with the fluid phase. Below $\phi = 0.49$ the fluid phase is stable, above $\phi = 0.545$, the crystal phase is stable. The crystallization of the HS arises from a delicate balance of entropy. In the fluid phase, disorder is associated to a larger number of configurations (large configurational entropy). Each of these configuration is characterized by a *rattling* entropy (the analog of the vibrational entropy in the case of continuous potentials), reflecting the available volume in which particles can rattle without leaving the configuration. Interestingly enough, the rattling entropy in the fluid phase is smaller than that in the crystal state, since disorder confines several particles in volumes significantly smaller than the crystal cage volume. The sum of the configurational entropy and the rattling entropy of the fluid at $\phi = 0.49$ equals the crystal rattling entropy at $\phi = 0.545$ and a crystallization transition takes place. The ordered crystalline state becomes more disordered than the disordered fluid state.

Among the possible crystal structures, the face-centered-cubic (*fcc*), hexagonal close packing (*hcp*) and body-centered-cubic (*bcc*) (the first two differing only for the stacking of different hexagonal planes) have the lower free energy (for a recent review see [73]). Among them, the lowest absolute one is provided by the *fcc* structure. The experimental study of the crystallization process in HS colloidal dispersions is an active field of research, revitalized by recent experiments in microgravity in order to eliminate the sedimentation, convection and stress due

to gravity [74–76]. Interestingly enough, experiments have shown that crystallites grow faster and larger in microgravity and the coarsening between crystallites is suppressed by gravity. Dendritic structures have also been observed to grow. Particularly important appears the experimental evidence that crystallization proceeds even for $\phi > 0.58$, a value for which, in normal gravity, no signs of crystal formations are observed even for extremely long observation times [77]. Computer simulation studies [78] confirm the role of gravity in affecting crystallization, suggesting that gravity appears to stabilize the glass state by reducing the mobility of the particles.

One important scientific question concerns the limit of stability of the fluid phase. Under appropriate experimental conditions, for finite experimental observation times the concentration of HS can be continuously increased beyond $\phi = 0.49$, generating a metastable fluid phase (metastable respect to the coexistence of a fluid at $\phi = 0.49$ and a crystal at $\phi = 0.545$). When the fluid properties are time-independent, the system can be properly considered as lying on the metastable extension of the fluid branch. On increasing ϕ , the time requested to reach a metastable equilibrium (i.e. when pressure does not change any longer) becomes comparable to the crystallization time and a proper extension of the metastable fluid branch cannot be further measured. Despite this undeniable difficulty which stops the observation of metastable equilibrium states at $\phi \approx 0.54$, several studies have addressed the issue of the large ϕ extrapolation of the metastable branch. Several researchers have argued that the metastable extension of the fluid equation of states predicts a divergence of the pressure around $\phi_{RCP} \approx 0.64$, a value historically identified with the random close packing state, i.e. the maximum density at which a random distribution of non-overlapping spheres can be generated. The pressure divergence at ϕ_{RCP} would correspond to the fluid analog of the divergence at $\pi/\sqrt{18} \approx 0.74$ which is the densest [79] possible packing fraction of spheres, corresponding to the close-packed *fcc* lattice or its stacking variants.

The utility of the concept of random close packing has been recently questioned by Torquato and coworkers [80], on the basis that configurations with any arbitrary packing can be generated with an appropriate amount of crystalline order. Indeed, in the absence of any thermodynamic condition, no unique property can be associated to HS configurations with $\phi \gtrsim 0.54$. Different preparation techniques, or different growth process in numerical simulations, may generate different realizations strongly differing in static and dynamic properties. For this reason, Torquato and coworkers have suggested to switch from the Random Close Packing (RCP) ill-defined concept to the Maximally Random Jammed state as the most disordered jammed state. In this case disorder is defined via an appropriate order parameter, and a jammed state is defined as a state in which all particles in the configurations are blocked by nearest neighbors contacts.

When HS configurations are generated at high packing fraction $\phi \gtrsim 0.58$, both experimentally by shear melting the crystal or numerically by compression algorithms [81, 82], the relaxation time of the system becomes much longer than the experimentally available time and the system behaves as a non-ergodic system. In particular, in experiments on earth, no signs of crystallization have been observed in the range $0.58 < \phi < 0.64$ (except for an extremely slow aging) leading to the hypothesis that, even for a one-component monodisperse HS system, a glass state

can be defined. The comparison with the zero gravity experiment confirms that these glassy states are metastable, as compared to the crystal state, and are kinetically stabilized by a growth of the crystallization time scale induced by gravitational effects. Still, around $\phi=0.58$ a change in crystallization kinetics has been reported [77, 83–86]. Support for the existence of an underlying ideal glass transition is offered by the experimental studies of the relaxation dynamics close to $\phi=0.58$. In the experiments, the presence of a small polydispersity (and possibly of the gravitational field) delays the crystallization process, allowing for the experimental measurements of the decay of the density fluctuations. The decay of the correlation functions (figure 2) shows the insurgence of a clear two-step relaxation process on approaching $\phi=0.58$. For $\phi > 0.58$, correlation functions do not decay to zero any longer within the experimental time window. The ϕ dependence of the characteristic time follows a power law dependence, consistent with the prediction of the ideal MCT. A recent refined analysis of the light scattering data based on the results of the full MCT, reported in [87], provides further support. A more thorough comparison of the entire t and ϕ dependence of the correlation function with the full solution of the ideal MCT equation, confirms the ability of MCT to model the shape and ϕ dependence of the dynamics close to dynamic arrest [88]. The presence of weak polydispersity and gravity is apparently fundamental in the experimental observation of the slowing down of the dynamics close to $\phi=0.58$. Indeed, simulation studies in zero gravity and in purely monodisperse systems cannot be performed close to $\phi=0.58$, since above $\phi \approx 0.53$ crystallization intervenes well before correlation functions have decayed to zero, preventing the calculation of any equilibrium dynamic property.

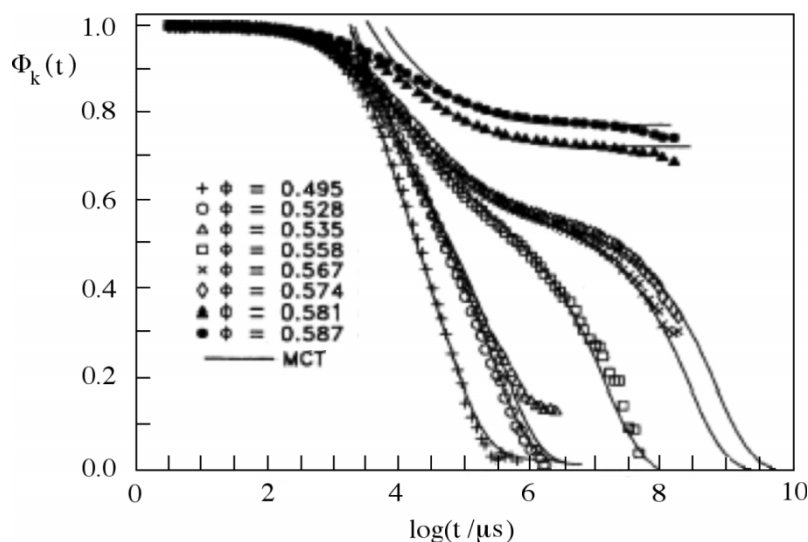


Figure 2. *Dynamic light scattering experiments in hard-sphere colloids.* The figure shows the intermediate scattering function for $kR = 4.10$ (k is the wavevector, R the particles radius) on increasing concentration. In scaled units, the maximum of the structure factor is located around $kR = 3.46$. The solid lines are MCT fits. Courtesy of the authors, redrawn from [85] with permission of the APS (American Physical Society).

Theoretical work based on the solution of the MCT equation using as input the static structure factor S_k calculated in the Percus-Yevick (PY) approximation, predicts an ideal MCT transition at $\phi_c = 0.516$. Close to ϕ_c , the relaxation time scales as $|\phi - \phi_c|^{-\gamma}$ with $\gamma = 2.52$ [89]. The exponent γ has been calculated first by Barrat *et al.* [90] (see also ref. [89]). A first test of exponents and scaling laws for HS was done by Götze and Sjögren [91] based on the pioneering work of van Meegen and Pusey [84]. As we mentioned earlier, exponents and critical laws are expected to be largely universal, while the actual value of the transition is significantly affected by the underlying approximation. Indeed, as alluded above, comparison with experiments confirms the quality of the theoretical predictions once experimental and simulation data are considered at the same relative distance from ϕ_c . Improvement on the S_k used as input to the theory (going from PY to Verlet–Weis [92] or to the *exact* S_k calculated in computer simulations of the HS model) does shift the estimate of ϕ_c up to 0.546 [93]. A recent extension of the MCT approach shifts ϕ_c to 0.549, although the agreement with the experimentally measured correlation functions is slightly worse [30]. The mean square displacement in colloidal HS has been studied with ingenious light scattering techniques by van Meegen *et al.* [94]. This quantity provides a precise and direct estimate of the onset of slow dynamics and of the particle cage, an important concept in the discussion of the glassy dynamics. A careful explanation of the mean square displacement data has been recently provided by Sperl [95].

Dynamics in HS systems in colloidal supercooled fluids and colloidal glasses have also been investigated in real space with laser scanning confocal microscopy [96, 97], a technique which provides the full three-dimensional trajectories of several thousand fluorescence labeled particles. It was found that particles moved cooperatively. These heterogeneities manifest themselves as a non-Gaussian probability distribution of particle displacements and affect the onset of long-time diffusive behavior. The characteristic size of the cluster of mobile particles grew markedly in the supercooled fluid as the glass transition was approached, confirming computer simulations results [98]. Again the glass phase [99] was also shown to be both spatially and temporally heterogeneous. Furthermore, while the characteristic relaxation time scale grows with the age of the sample, nontrivial particle motions continue to occur on all time scales. The same technique has also been used to study crystallization of concentrated colloidal suspensions [100]. Direct imaging in three dimensions allowed the identification and observation of both nucleation and growth of crystalline regions, providing an experimental measure of properties of the nucleating crystallites. The structure of the nuclei was found to be the same as the bulk solid phase, random hexagonal close-packed, and their average shape was rather non-spherical, with rough rather than faceted surfaces.

In the spirit of MCT, the ideal glass transition is a kinetic transition, completely disconnected from any thermodynamic one. Extending the theory to include hopping effects (which in a first approximation may not play a significant role in HS systems), could explain the residual mobility beyond $\phi = 0.58$, consistent with the observed extremely slow decay of correlation functions above ϕ_c and the crystallization observed in the zero gravity experiments. Instead, other theories suggest the presence of a real thermodynamic transition on increasing ϕ , related to the vanishing of the configurational entropy, defined as the number of explored distinct disordered

configurations. Speedy [101] studied the thermodynamic properties of HS fluids and their glasses, using molecular dynamics simulations, describing them within a unified formalism, by expressing the number of configurations of a fluid as a sum, over all its glasses, of the number of configurations of each glass. For pure HS and mixtures of HS this approach provides an equation of state that interpolates between the ideal gas low density limit and an ideal glass high density limit, and includes a thermodynamic glass transition. On a finite time scale, a real glass transition pre-empts the ideal one. The ideal glass transition is predicted around $\phi = 0.657$, at which point the specific heat shows a discontinuity. Speedy also notes that the entropy of the glass at the ideal glass transition is different from the crystal entropy at the same temperature and pressure, due to the difference rattling entropy of the two states, this time both of them characterized by the same configurational entropy. Recent calculations are consistent with Speedy's findings [102].

A similar conclusion is reached by Cardenas and coworkers [45, 103], who studied the glass transition for simple liquids in the HNC approximation by means of an effective potential, recently introduced. Integrating the HNC equations for HS, they find a transition scenario analogous to that of long-range disordered systems with one-step replica symmetry breaking. These results have been extended in a recent work of Parisi and Zamponi [104]. Finally, Aste and Coniglio [105] developed an approach that combines the ideas of inherent structures, free volume theory and geometrical packing properties. When applied to HS systems, the theory describes the critical approach toward the random close packing density, with the configurational entropy that approaches zero.

3.2. Polydisperse hard spheres

One possible mechanism to hamper crystallization is provided by disorder in the particle sizes, inducing concomitant disorder in the interparticle potential. Above a certain polydispersity of about 7% a crystalline phase does not usually exist, while slowing down of the dynamics is certainly observed. In this respect, the glass dynamics does not require metastability with respect to a crystal phase. In experimental samples, an intrinsic polydispersity (of the order of a few percent) induced by the preparation techniques, is often present. Especially in numerical studies, polydispersity is induced under controlled conditions to be able to study packing fraction values at which the monodisperse HS system inevitably crystallizes, significantly extending the interval of explored time scales.

Binary mixtures of simple particles have been used, since the work of Hansen and collaborators [106], for numerical studies of the glass transitions, as a way of suppressing crystallization. More recently, experiments [107], theory [29] and simulations [93, 108] have addressed the effect of mixing on structural relaxation to identify the influence of composition changes and variation of the particle size disparity on the HS glassy dynamics. In the experimental work of Williams and van Meegen [107] three mixing effects have been reported. If the percentage of the smaller particles increases from 10 to 20% of the relative packing fraction, then (i) the time scale for the final decay of the density correlators decreases; (ii) the plateau value for intermediate times increases and (iii) the initial part of the structural relaxation slows down. The first effect means that mixing has promoted the liquid

as if the smaller particles provide some lubrication. This effect has some analog in the plasticization observed in dense polymeric liquids due to mixing with polymers of shorter lengths. However, effects (ii) and (iii) indicate a stiffening of the dynamics upon mixing. Theoretical work [29] has identified these phenomena as structural relaxation effects rather than colloid-specific features. It suggests moreover that the speed up of the dynamics reported in [107] is characteristic only of sufficiently large size disparity, predicting the opposite effect (i.e., mixing slows down the dynamics and the ideal-glass critical packing fractions decrease) for smaller size ratio. Theoretical predictions have been confirmed by numerical simulations [93, 108]. Simulation results provide evidence that increasing the mixing percentage of the smaller minority particles can lead to a speeding up, as well as to a slowing down, of the long-time decay processes, depending on whether the size disparity is large or small, respectively. There is also an increase of the height of the plateau of the density autocorrelation functions for small and intermediate wave vectors, reflecting a stiffening of the nearly arrested glass structure. These findings, which pose a challenge to theories of the glass transition, show, in particular, that the description of a glass-forming mixture by an effective one-component liquid cannot be possible for all properties of interest. Due to the suppression of crystallization phenomena, the comparison between simulation and theoretical predictions in binary mixtures can be performed in a punctual way. Indeed simulations can be extended over five orders of magnitude in dynamic range, without any sign of crystallization. In these conditions, indications of slow dynamics are rather clear and allow researchers to provide high quality data. In the case of binary HS systems, the wavevector dependence of the non-ergodicity parameter has been found to closely describe the theoretical predictions, once the *exact* numerical partial structure factors are used as input in the theory, as shown in figure 3. We refer to ref. [23, 87, 93, 108] for a thoughtful comparison between MCT predictions and simulation results for the binary HS system.

A significant influence of gravity on the long-time behavior of the mean squared displacement in glasses of polydisperse colloidal HS was reported in an experimental study, based on real space fluorescent recovery after photobleaching [109]. Systems which are glasses under gravity (with a gravitational length on the order of tens of micrometers) show anomalous diffusion over several decades in time if the gravitational length is increased by an order of magnitude. No influence of gravity was observed in systems below the glass transition density. It appears that gravity dramatically accelerates aging in colloidal HS glasses. This behavior is consistent with the observation that colloidal HS systems which are a glass on Earth rapidly crystallize in space [74–76].

Highly polydisperse HS systems have been recently studied to address the question of a possible thermodynamic transition associated to the slowing down of the dynamics. For the case of two-dimensional polydisperse HS, Santen and Krauth [110] have designed a clever Monte Carlo cluster algorithm which makes it possible to equilibrate the system under high packing fraction conditions, finding no evidence of a thermodynamic transition. Unfortunately, the significant presence of polydispersity does not settle the issue once and for all [80].

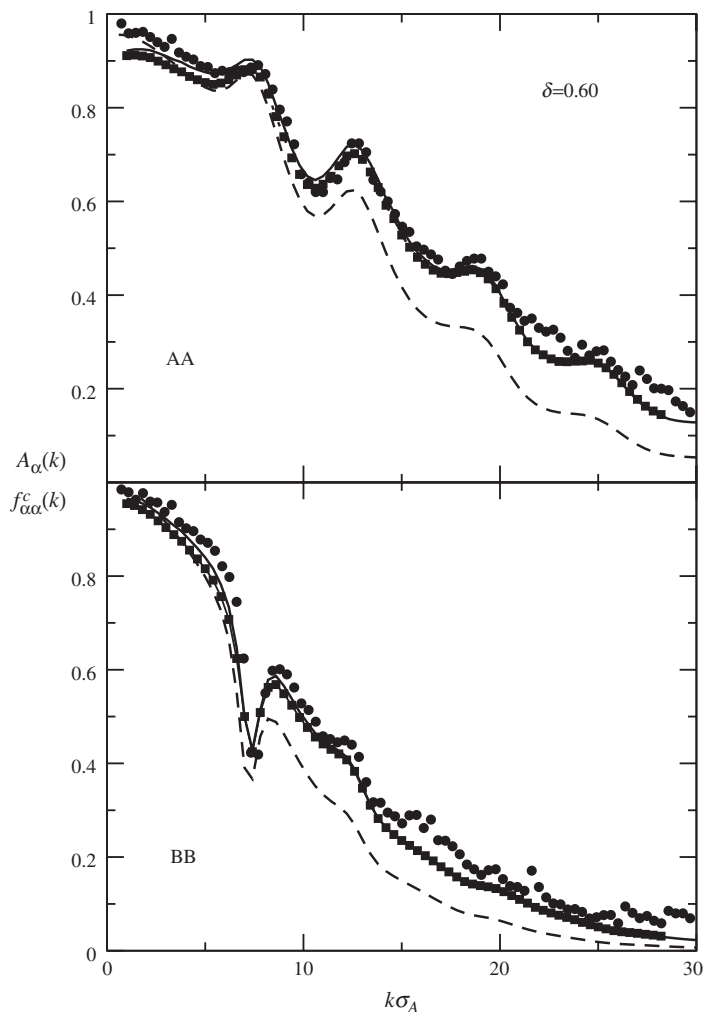


Figure 3. *Non-ergodicity parameter for binary HS systems.* This figure shows results from a event driven simulation of a binary mixture of particles A and B, with B/A size ratio of $\delta = 0.60$. Circles and squares represent the Kohlrausch amplitudes $A(q)$ determined by fitting the α -relaxation decay to the equation $\phi(q, t) = A(q) \exp[-(t/\tau(q)^\beta)^{\beta}(q)]$ to the simulation data and to numerical solutions of the MCT equations for the normalized autocorrelation functions. Results for the big particles A are in the top panel, while for the small particles B in the bottom panel. The solid and dashed lines show the MCT plateau values calculated using respectively as input the structure factor evaluated from the simulation data and from the Percus-Yevick approximation. Redrawn from [93] with permission of the APS.

3.3. Hard ellipsoids

An interesting class of hard particles which is receiving considerable interest is constituted by hard ellipsoids of revolution, the simplest extension of the HS case

toward non-spherical interactions. The phase diagram of this system [111] is a function, beside packing fraction, of the ratio $x \equiv b/a$ ($0 < x < \infty$), where a and b denote the length of the major and minor axis of the ellipsoids. Oblate and prolate ellipsoids are respectively described by $x < 1$ and $x > 1$. At low ϕ , the phase diagram includes an isotropic phase bounded by nematic phases both at large and small x [111–113]. In the nematic phase, orientational order is long-range, while translational center of mass order is short ranged. At large ϕ translational ordered phases are found, with plastic features (orientation disorder) for $x \approx 1$.

The slow dynamics in hard ellipsoids has been characterized within molecular MCT [114] using as input static orientational correlation functions evaluated via PY closure [113, 114]. The resulting kinetic phase diagram is reproduced in figure 4. The slowing down of the ellipsoids in the isotropic phase is predicted to take place via two different mechanisms: one is the usual mechanism related to caging, as found also in the HS case, the second one is a slowing down driven by the angular degrees of freedom, which takes place close to the nematic transitions. Experimental and/or numerical evidence for this second additional mechanism is still missing, and is one of the open challenges in this field. In both mechanisms, translational–rotational coupling is sufficiently strong to produce a simultaneous

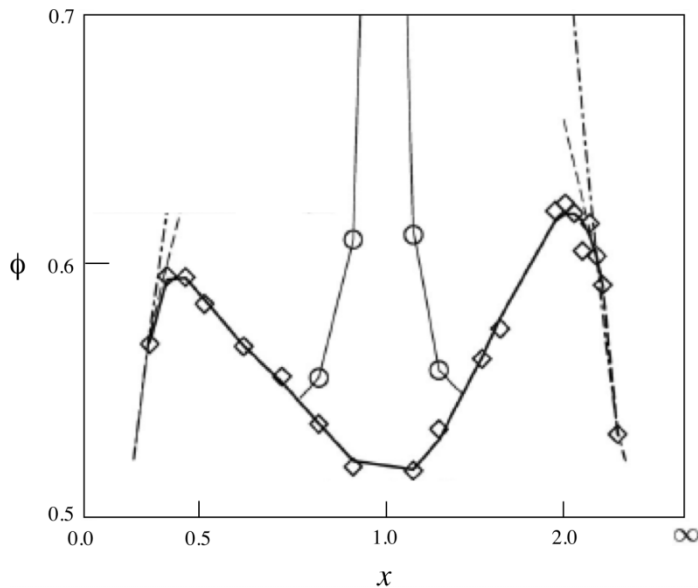


Figure 4. *Phase diagram for the ideal glass transition of hard ellipsoids.* The horizontal axis shows the aspect ratio $x = b/a$ (b and a major and minor axis of an ellipsoid of revolution) scaled with $(x^2 - 1)/(x^2 + 1)$. In this system, two different types of glass lines (type A and type B) are predicted, differing from the evolution of the non-ergodicity parameter at the transition, evolving continuously from zero in type A transition and discontinuously in type B. The type B glass transition lines are depicted as thick solid and dashed lines. The thin solid line is the A glass transition line. Note that an enlargement of the intersection would show that the type A line meets the B line tangentially. The figure shows also the location of the nematic instability (as evaluated from the PY theory) as thin dashed-dotted lines. Redrawn from [114]. Courtesy of the authors, with APS permission.

freezing of both orientation and translation dynamics. An additional glass transition line is also predicted for nearly spherical ellipsoids, where the orientational degrees of freedom with odd parity (i.e. 180° flips) freeze independently from the position, with a type A-MCT transition [114].

A detailed MCT study of the dynamics of hard dumbbells as a function of the dumbbell elongation, in the site–site representation [115, 116], shows a behavior similar to the one predicted for nearly spherical ellipsoids in [114]. Figure 5 shows the predicted theoretical phase diagram for dumbbells. Similarly to the ellipsoid case, below a critical elongation, center of mass and odd orientational degrees of freedom decouple, giving rise to a plastic phase which ends, on increasing packing fraction, at a type A transition. Evidence for this scenario has been recently provided by numerical simulations [117, 118].

Both the molecular MCT for the case of hard ellipsoids and the site–site MCT for the case of hard dumbbells, suggest a non-monotonic behavior of the critical packing fraction, with a maximum at intermediate values of the asymmetry [114–116]. Recent experimental studies on systems with *elongated* particles, like ellipsoids [119] and spherocylinders [120], have revealed that the random (amorphous) jammed packing is characterized by a maximum attainable packing fraction ϕ_{\max} , which is a non-monotonic function of the elongation parameter which characterizes the shape of the particles [119, 120]. Starting from $\phi_{\max} \approx 0.64$, the value for random close packing of hard spheres, ϕ_{\max} reaches a maximum $\gtrsim 0.70$ at intermediate elongations and then

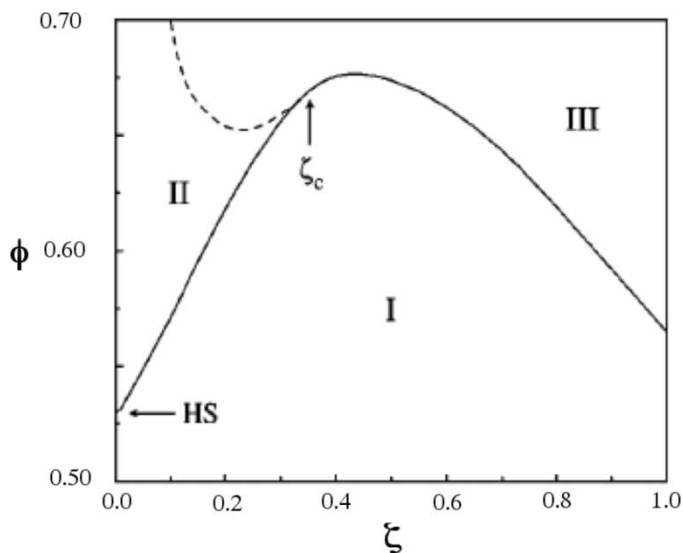


Figure 5. *Ideal MCT glass transition locus for the symmetric hard dumbbell system in the packing fraction ϕ -elongation ζ plane.* As in the ellipsoid case, a type A and a type B transition are predicted, partitioning the phase diagram in three regions. The solid curve marks the type B liquid-glass transition line. The dashed curve denotes the type A transition line between phases II and III. The type A transition line terminates at the critical elongation $\zeta_c = 0.345$, marked by an arrow. The horizontal arrow marks the transition point of the HS system. Redrawn from [116]. Courtesy of the authors, with APS permission.

decreases again for larger ones. The similarity between the shape of the crystallization line, the MCT ideal glass line and the ϕ_{\max} line in the ϕ -aspect ratio plane suggests a common origin for all these observations, an issue which will deserve further debate and which may provide an explanation of the experimental findings in terms of MCT. The increase of maximum attainable packing fraction in disordered states observed in hard ellipsoids, as compared to the case of HS, is a characteristic not only of the disordered state but also of the crystal state. Indeed, while the maximum packing fraction of the HS is 0.7405, in the case of ellipsoids a recent study [121] reports a maximum packing fraction up to 0.7707 for aspect ratios larger than $\sqrt{3}$, when each ellipsoid has 14 touching neighbors.

4. Attractive colloids

In most cases, colloid–colloid interactions are characterized not only by the hard-core excluded volume interaction, but also by an additional one, arising from the polarizability of the particle and from the chemistry of the particle surface. The strength and range of these interactions is modulated by the solvent properties (temperature, salt concentration, pH, solvent composition). The effective colloid–colloid interaction can also be controlled by the addition of a third component (beside colloid and solvent), which acts as depletant agent. Often, the range of the interaction is significantly smaller than the particle size, giving rise to interparticle effective potentials that have no counterpart in atomic or molecular systems.

An interesting case is generated when the hard core potential is complemented by an attractive potential, the range of interaction of which is significantly smaller than the colloid size. The addition of an attractive component introduces the possibility of a separation into coexisting colloid-rich and a colloid-poor phases, when the interaction strength overcomes a critical value. The separation of the homogeneous solution into two coexisting phases is the analog of the liquid–gas coexistence in a one-component atomic or molecular system. Contrary to the atomic or molecular liquid cases, for which the interaction range is always comparable to the particle size, in the case of very short-ranged potentials the two-phase coexistence is located on the metastable extension of the fluid free energy and technically no triple point (crystal, liquid, gas coexistence) exists [122]. Coexistence of fluid and crystal phases is the equilibrium state. Indeed, it is found that the critical interaction strength (i.e. the strength at which the second-order colloid-rich colloid-poor critical point is located) decreases on increasing the range of interaction [122–135]. Only when the interaction range becomes approximately 20% of the colloid diameter [135], the critical point emerges into the stable fluid phase and a proper equivalent of the equilibrium liquid phase can be defined [136]. A pictorial representation of the evolution of the phase diagram on increasing the range of interaction is shown in figure 6 [122].

The addition of an attractive part to the HS potential brings in the possibility that slowing down of the dynamics can be driven not only by the increase in packing (the ϕ -route), but also by an increased role of the attraction between different particles (the T -route). The possibility of going continuously from the HS case to the atomic case by progressively increasing the range of interaction, has motivated

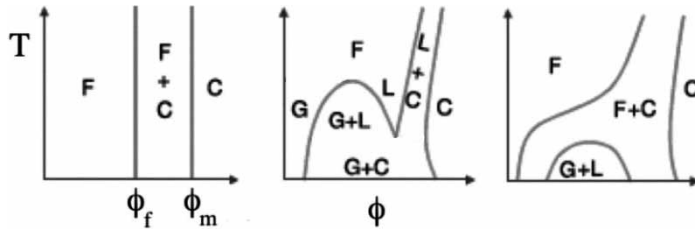


Figure 6. *Pictorial representation of the phase diagram of colloidal particles.* The first panel refers to hard spheres, where freezing occurs at $\phi_f = 0.494$, melting at $\phi_m = 0.545$. The middle panel shows the appearance of the liquid–gas coexistence, and the associated critical point, when an attractive potential is added to the hard-sphere repulsion. The last panel shows the disappearance of the liquid phase, which becomes metastable when the range of the interaction becomes sufficiently short ranged. Phases are labelled as follows: fluid (F), crystal (C), gas (G) and liquid (L). Redrawn from [122], courtesy of the authors, with permission from *Nature Publishing Group*.

in the last decade a relevant number of studies, which have provided an extensive and unifying picture of the slow dynamics in fluid systems, either colloidal or atomic and molecular.

4.1. MCT predictions

The first theoretical analysis of the role of a short-ranged attractive potential in the dynamics of colloidal suspension was presented in two seminal MCT studies [137–139]. These studies showed that the arrest of density fluctuations can either be dominated by repulsion of the particle by its cage-forming neighbors (as in HS systems), but also by the formation of bonds (energetic cages) between particles. The original calculations, based upon Baxter’s adhesive HS model [140] (with a suitable cut-off at large wavevectors to account for the unphysical divergence due to excitations with large wave vectors), were confirmed by more refined calculations based on the square-well (SW) model [141]. The interaction SW potential $V(r)$ for particles with separation distance r consists of a hard-core repulsion for $r < \sigma$, and it has the negative value $-u_0$ within the attraction shell $\sigma < r < \sigma + \Delta$. The SW kinetic MCT phase diagram is reproduced in figure 7. The *unexpected* theoretical predictions resulting from these analysis included the following.

- (i) The possibility of melting a HS glass by progressively switching on an attractive interaction with a range smaller than about one-tenth of the particle diameter. In the case where attraction is induced by depletion mechanisms, theory predicts a melting of a glass by further addition of a third component.
- (ii) The vitrification of the melted HS glass upon further increase in the attraction strength.
- (iii) The possibility of generating liquid states at packing fractions significantly higher than the packing fraction at which the HS system arrests.
- (iv) A non-monotonic behavior of the characteristic structural times as a function of the attraction strength.
- (v) The possibility of a sharp transition between the HS and the bonding localization mechanisms, for very small ranges of attractions. The transition

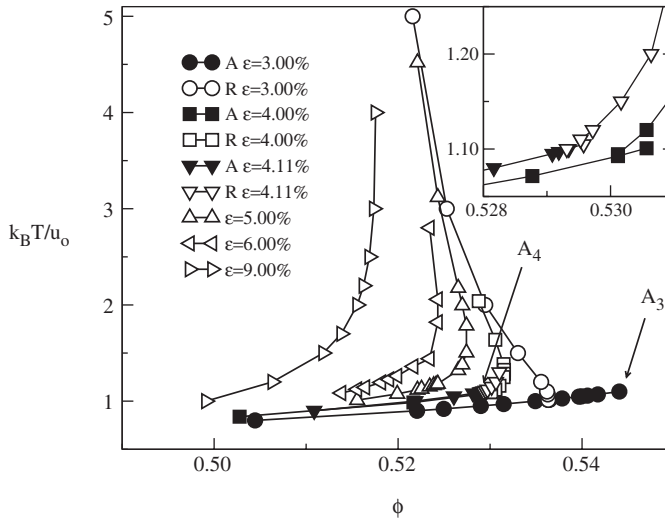


Figure 7. *The ideal MCT phase diagram of the square well system.* The phase diagram shows cuts through the control parameter space, volume fraction ϕ and ratio of temperature to well depth $k_B T/u_0$, for fixed relative attraction well width $\epsilon = \Delta/(\sigma + \Delta)$ ranging from 3 to 9%. The re-entrance of the glass lines appears only for $\epsilon < 0.09$ and extends the range of existence of the liquid phase. Below $\epsilon \approx 0.04$ the glass–glass line appears and increases its length as ϵ decreases. For these small values of ϵ two different solutions are found, commonly named the repulsive (*R*) and the attractive (*A*) one. The inset highlights the location of the A_4 higher-order singularities. The A_3 point is the terminus of the *A* line, while the A_4 point marks the location where the *R* and *A* lines join continuously and it is the only higher-order singularity accessible from the equilibrium liquid. Redrawn from [141], with APS permission.

is accompanied by a discontinuous changes of the elastic properties of the glass.

- (vi) A decay of the density correlation function utterly different from the one characteristic of the HS system, in the region where the two different localization mechanisms compete with comparable strength [142, 143].
- (vii) The possibility of observing, for a specific choice of the interaction range, a fully developed logarithmic decay of density fluctuations (a higher-order singularity in the MCT classification scheme) [142, 143].

The basic physics behind these phenomena results from a competition between two different mechanisms constraining the particle motion. To grasp the origin of this competition, consider the HS system. When the volume occupied by the HS becomes larger than 58% of the available volume, structural arrest is observed. In the resulting glass, particles are hindered from moving too much by the presence of neighboring ones, and are *caged* by their neighbors. Only an extremely rare collective rearrangement, for example opening a channel out of the cage, makes particle diffusion possible. In such packed conditions, particles can only rattle within their own cage, getting no further than an average distance of around 0.1σ . In the presence of an additional short-range interparticle attractive interaction something different takes place. At high temperature, the attraction does not play any role and, if the

volume fraction occupied by the particles is large enough, the material will behave pretty much like a HS glass. But if the range of the attraction Δ is smaller than 0.1σ , then on cooling particles will begin to stick together, effectively shrinking the confining cage size and producing a more inhomogeneous distribution of the empty space. The structure factor of the system reflects these changes. The height of the first peak decreases while the small wavevector value, a measure of isothermal compressibility and hence of the density fluctuations, increases. These empty regions form channels through which particles can diffuse and so the material starts to melt. As a result, the glass turns into a liquid on cooling. If the temperature is further lowered, interparticle bonding will become strong and longer lasting, thereby restoring the usual progressive slowing down of dynamics, which results in another structural arrest. The liquid turns back into a glass. In the temperature–volume fraction phase diagram, this glass–liquid–glass sequence results in a re-entrant (non-monotonic) glass transition line. It also means that some liquid state can be stabilized by the short-range attraction, and so – compared to the long-range attraction case – the range of stability of the liquid phase is increased. Within the MCT, the glass–fluid–glass transition arises from the progressive changes of the structure factor, the only input of the theory beside the (constant) number density. The HS glass, stabilized by the large value of the first peak of the structure factor, melts due to the weakening of the structure factor in the first peak region. The new glass transition is instead driven by the increased large wavevector oscillation (arising from the well defined bonding length and to the bonding localization). The phenomena we just described are summarized in the schematic sketch of figure 8.

A significant experimental and numerical body of work has attempted to check the theoretical predictions and/or reinterpret previous results in the frame set by MCT calculations. The most thorough investigation is based on a dense systems of colloidal particles, characterized by a hard core and strong attraction of a range smaller than the core diameter by a factor of at least 10, realized experimentally, when adding non-adsorbing polymers to a suspension of colloidal HS. In this case, an entropic generalized force is produced, related to the different volume accessible to the polymer when its center of mass is located between two colloidal particles, compared to the condition when the polymer is not constrained by the colloid. The Asakura–Oosawa model [145] is conventionally used to present the equilibrium phase behavior of colloids containing non-adsorbing polymers. According to this model, colloidal particles are represented by HS and polymers by ideal chains that do not interact with each other. While the ideal polymer chains are allowed to interpenetrate, they are excluded from the particle surface, i.e., the center of mass of a polymer chain is located from the particle surface at a distance no closer than the polymer radius of gyration. Due to the entropy effect, the excluded volume of the ideal polymers results in an effective attraction between colloidal particles, which can be represented by the Asakura–Oosawa potential $V^{AO}(r)$. This potential is zero for distances (between the colloidal particles' centers) $r > \sigma + \sigma_p$, where σ is the colloid diameter and σ_p is twice the polymer gyration radius. For $r < \sigma + \sigma_p$

$$\beta V^{AO}(r) = -\phi_p \left(\frac{1+\delta}{\delta} \right)^3 \left[1 - \frac{3}{2(1+\delta)} \frac{r}{\sigma} + \frac{1}{2(1+\delta)^3} \left(\frac{r}{\sigma} \right)^3 \right]$$

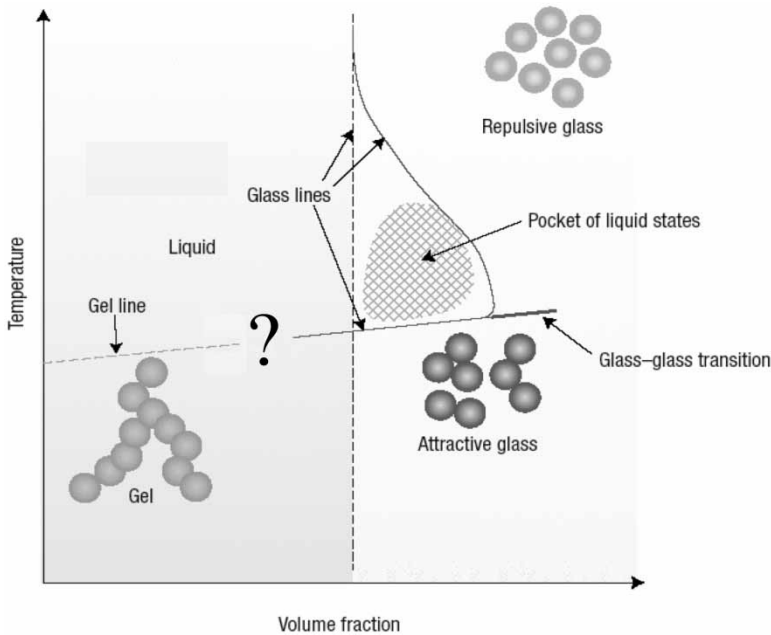


Figure 8. *Schematic phase diagram of a colloid with hard-sphere interactions complemented by a short-range attractive part.* Two intersecting glass lines are observed, separating the metastable supercooled liquid by the repulsive and attractive glasses. At high temperatures the repulsive glass line approaches the hard-sphere one. The repulsive glass is dominated by cage effects driven by the excluded volume. At lower temperatures the repulsive glass line moves to higher volume fractions and gives rise to a pocket of liquid states. At low temperatures there is an attractive glass line. The attractive glass is dominated by cage effects driven by the short-range sticky interactions. The attractive glass line generates at high ϕ a glass–glass line along which the elastic properties of the glass change discontinuously. At much lower ϕ , a gel line is experimentally observed. The connection between the gel line and the attractive glass line is object of ongoing research. Reproduced from [144], with permission from *Nature Publishing Group*.

where $\phi_p \equiv (\pi/6)\sigma_p^3 n_p$ is an effective packing fraction of the depletants, with number density n_p . The Asakura–Oosawa potential was originally obtained from geometric considerations but it can also be derived from statistical mechanics [146] under the assumption $\sigma_p/\sigma \lesssim 0.1547$ [147]. According to this potential, the strength of attraction between colloidal particles is controlled by the polymer packing fraction and the range of attraction by the polymer radius of gyration. Various statistical mechanical theories for representing the thermodynamic properties of AO fluids have been recently reviewed by Poon [148].

4.2. Experiments

In the work of Pham and colleagues [7, 149], the investigated sample was composed of stabilized PMMA particles (HS radius $R = 202$ nm, polydispersity 7%) dispersed in cis-decalin, a well-characterized HS sample. A short-range attraction was induced by adding a non-adsorbing polymer, polystyrene (radius of gyration 17.8 nm).

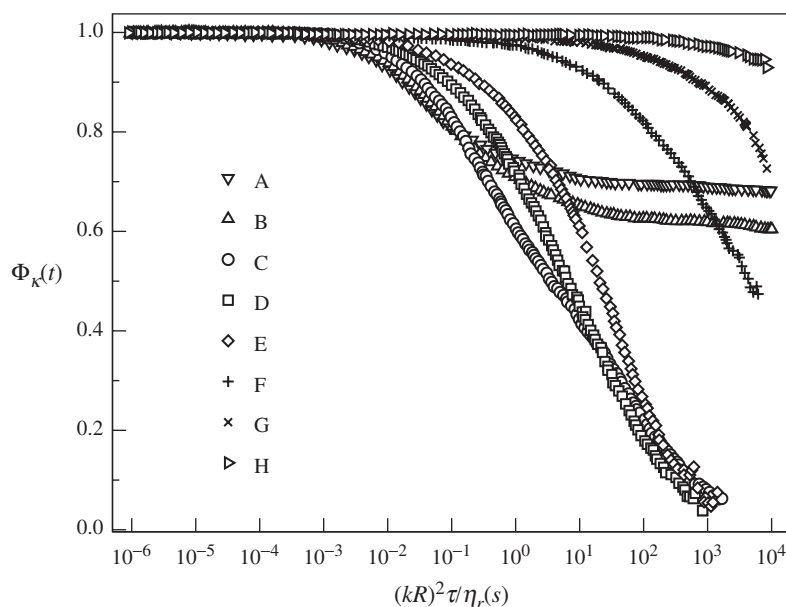


Figure 9. *Light scattering correlation functions for a hard-sphere colloid system in the presence of depletion interactions.* The figure shows the intermediate scattering function at $kR = 1.50$ for a PMMA sample at constant ϕ on increasing polymer concentration (from A to H). The actual values of the concentration of depletant are reported in [149]). On increasing depletant concentration, the correlation function becomes first faster and then slows down again approaching again structural arrest, signaling a non-monotonic dependence of the characteristic time. Note also that the height of the plateau (the non ergodicity parameters) changes from values characteristic of HS ($f_q \approx 0.6$) to much larger values characteristic of the attractive glass ($f_q \approx 1$). The time axis is scaled with kR and the relative polymer solution viscosity η_r . Redrawn from [149]. Courtesy of the authors, with APS permission.

The dimensionless range of the depletion attraction was estimated to be 0.09. The experimental study of the particle dynamics reveals a re-entrant glass transition (figure 9). With little attraction, the system at high enough volume fraction is *stuck* in a repulsive glassy state, where the arrest is due to caging by neighboring particles. The data clearly support the suggestion that attraction causes particles to cluster, thus opening up holes in the cages and melting the glass. Increasing the attraction further leads to different kind of arrest, where the strong attraction between particles creates long-lived bonds and prevents structural rearrangement, giving rise to an attraction-dominated glass. Detailed light scattering experiments, used to probe the effect of attraction on both structure and dynamics, confirmed the differences in the shape of the density autocorrelation functions and the different localization lengths characteristic of the two glasses. Experiments [149] were also able to detect a very slow, long-time dynamics in the re-entrant region where the two glass transition lines are expected to meet, providing full support to the theoretical predictions. Experiments also showed differences in the aging dynamics of the two different glasses, a feature which cannot be easily studied theoretically, but which has

been confirmed numerically [150], and which calls attention to the role of activated processes for the final decays of the dynamics in the attractive glasses and their aging behavior, a topic which requires further studies.

The first hint of the presence of a higher-order singularity in an attractive colloidal suspension was found in a copolymer–micellar system [151], where dynamic percolation and structural arrest transitions coexist in different regions of the phase diagram. The intermediate scattering function, reproduced in figure 10, showed a non-ergodic transition along a temperature and concentration dependent line. Analyses showed a logarithmic time dependence, attributed to a higher-order glass transition singularity of type A_3 as predicted by MCT, followed by a power law. These effects were tentatively related to short-range intermicellar attraction.

One of the first evidence for the MCT scenario for short-range attractive potentials was provided by a study of a binary mixture of polystyrene micronetwork spheres, swollen in the good isorefractive solvent (2-ethyl-naphthalene), of radius 150 and 185 nm respectively. The polymer chains within the particles are highly cross-linked so that particles can be reasonably well approximated as HS [152–154]. The colloid packing fraction was kept constant to 0.67, where a repulsive glass, consistent with the HS dynamics is found. In order to introduce short-ranged attractive interactions, linear polystyrene chains were added as a depletant, resulting in an interaction range $\sigma_p/\sigma \approx 0.054$. The measured density autocorrelation functions clearly showed a non-monotonic dependence on ϕ_p , showing non-ergodic states

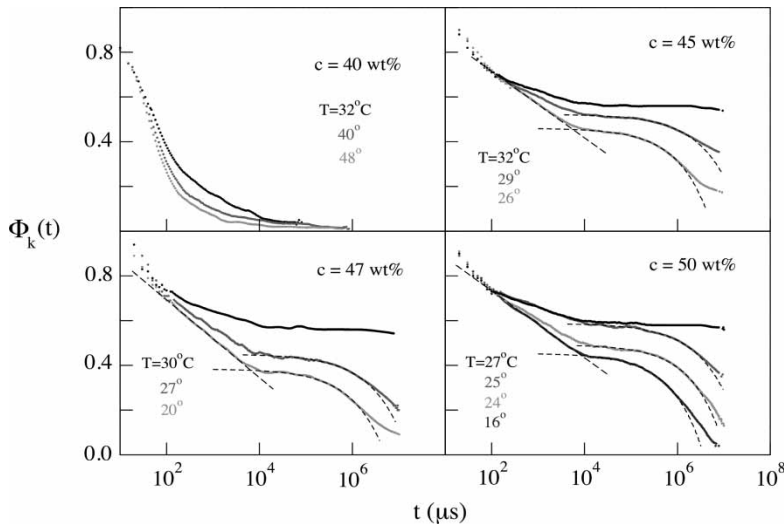


Figure 10. *Light scattering correlation functions from a triblock copolymer systems.* Density correlators for various concentrations of the dispersed phase and temperatures (listed in the panels from top to bottom) in the glass region of a copolymer–micellar system. At low concentration c (top-left panel), no signatures of slow dynamics are observed. On increasing c , the system develops a plateau, followed by a decay for longer times, which is well described by the von Schweidler power-law in time (short-dashed lines). For shorter times the intermediate scattering functions show, at lower temperatures, a logarithmic decay (long-dashed lines). The latter has been interpreted as an effect of a nearby A_3 higher-order singularity. Redrawn from [151], with APS permission.

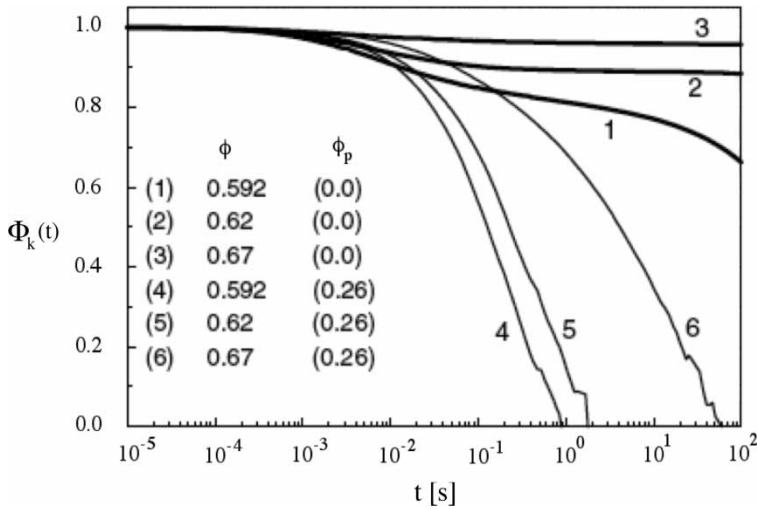


Figure 11. *Re-entrant behavior detected with scattering from micronetwork spheres in the presence of a depletant agent.* Comparison of the density autocorrelation functions of a micronetwork spherical colloidal suspension before (thick solid lines) and after (thin solid lines) the addition of linear polymer chains with volume fraction $\phi_p = 0.26$ (size ratio of polymer to colloid is 0.054). The colloid volume fraction ϕ of each set increases from left to right as indicated in the figure. The dynamics is probed at a scattering vector corresponding to the peak of the structure factor of the pure colloid suspension at its glass transition volume fraction of 0.595. The attraction causes the system to make a transition from glass to liquid state. Redrawn from [152], courtesy of the authors, with APS permission.

both at low and at high ϕ_p . The shape of the correlation function, reproduced in figure 11 for two different ϕ_p values. It is worth noticing that an experimental study of the same system had already evidenced the presence of a logarithmic decay of the density autocorrelation functions, which had been interpreted in terms of higher-order MCT transition [155–158].

Several following studies have provided further confirmations of the lubrication phenomenon induced by the short-range attraction, and the different dynamics of repulsive and attractive glasses [8, 159–161]. Particularly interesting is the case of a copolymer–micellar system with a short-range interparticle attractive interaction, studied by Chen and coworkers [8, 161]. Within a certain range of micellar volume fractions, a sharp transition between two types of glass has been observed by varying the temperature. Furthermore, an end point of this transition line, beyond which the two glasses become identical in their local structure and their long-time dynamics, has been detected. However, differently from the theoretical case which predicts that the glass–glass transition is essentially isostructural, in the experiments the different glass dynamics is associated to an abrupt change of the structure factor.

Rheology and dynamics measurements of a micellar solutions of polystyrene-poly(acrylic acid) block copolymers at large packing fractions provide another important example of a reentrant transition in the dynamics, and of the presence of higher-order MCT singularities [4]. In this system, attraction is increased progressively by controlling the percentage of stickers in the micelle corona. On increasing attraction, the elastic modulus G' first decreases and then increases again, while the

system progresses from the repulsive to the attractive glass. In the region where G' has a minimum, the particle dynamics shows a remarkable extended logarithmic decay, covering more than four orders of magnitude in time.

4.3. Numerical studies

A strong confirmation of the MCT theoretical predictions has been provided by accurate numerical studies of the slow dynamics in models of short-range attractive colloids [161–165]. The first results, provided by Puertas and coworkers [162, 163], focused on a polydisperse system of particles interacting via the Asakura–Oosawa potential, complemented by repulsive interaction (extending up to 2σ) to prevent the colloid-rich colloid-poor phase separation. Numerical calculations provided a clear evidence of the two different localization mechanisms, in close agreement with experimental results. Evidence of the anomalous dynamics was also provided by a study of the isodiffusivity curves in a one-component SW potential in the (ϕ, T) plane [164]. Irrespective of the sharp intervening of crystallization, which effectively prevented the system to approach very closely the glass transition, it was possible to have a clear picture of the reentrant shape of the glass curve in the temperature-density plane. This was achieved by plotting isodiffusivity curves and examining their trends when approaching the limit $D \rightarrow 0$. The shape of the isodiffusivity curves indeed provides indication of the shape of the ideal glass transition line, which can be considered as the zero iso-diffusivity locus. This study provided evidence of a re-entrant shape of the diffusivity line, in agreement with the MCT prediction. The study of the slow dynamics in a wider range of T and ϕ values required the extension to a binary mixture SW model, to prevent crystallization [165]. The choice of a two-component system makes it possible to extend the range of isodiffusivity curves to almost three decades, as well as the range of studied packing fractions from 0.57 for one-component to 0.62 for binary systems. The shape of the isodiffusivity lines in the (ϕ, T) is shown in figure 12. The resulting binary model may be regarded as canonical for interpreting the dynamical arrest. The accurate numerical study confirmed the theoretical predictions for re-entrance, logarithmic singularity and provided a direct evidence of the existence of two distinct glasses. The simulation clearly shows that when repulsive interactions dominate the classical arrest scenario is observed, in which plateaux develop as arrest is approached. These plateaux indicate the development of an observable characteristic cage time, and are quite typical of MCT predictions for HS systems. In the re-entrant region, the mean square displacement and the density correlators were found to exhibit an unconventional decay, which was interpreted as evidence of a nearby higher-order MCT singularity, the pattern of evolutions being essentially in agreement with the predictions of the theory. The numerical study also provided evidence of an abrupt change of the non-ergodicity factors along the arrest curve, a strong evidence of a transition from a repulsive to an attractive glass, again in line with theoretical predictions. An important point raised by the numerical study is the strong systematic shifts of all the MCT arrest curves in relation to the simulated ones, a phenomenon long known from the example of the HS. While at high T (the HS case) the shift between theory and simulation is of the order of 15% in ϕ , it becomes significantly larger (up to 300% in T)

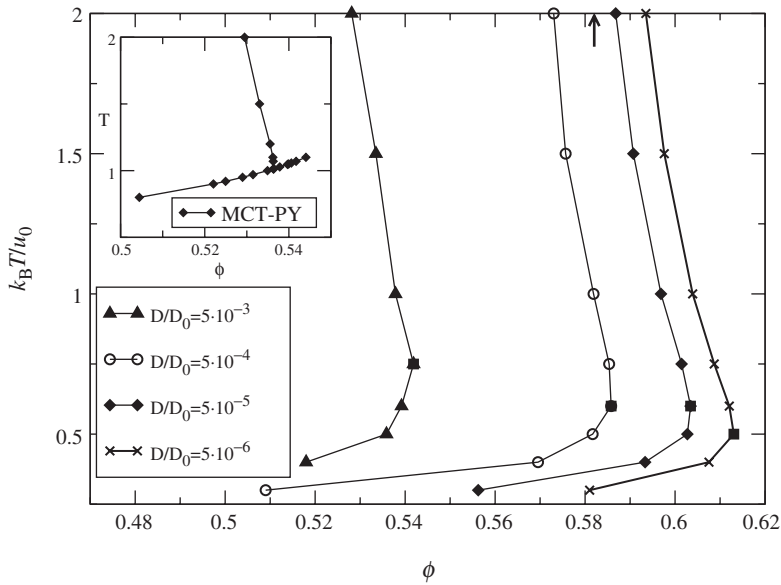


Figure 12. Simulated iso-diffusivity lines for the short-range square well system, for the determination of the glass line(s). The curves of iso-normalized-diffusivity D/D_0 (with $D_0 = \sigma_A \sqrt{T/m}$) in the volume fraction vs. temperature plane, obtained by event-driven molecular dynamics, provide an indication of the shape and location of the line of structural arrest. The vertical arrow provides the infinite temperature limit for the lowest iso- D/D_0 curve, i.e., $D/D_0 = 5 \times 10^{-6}$, corresponding to the hard-sphere case. Along each curve, the corresponding most reentrant point is represented with a filled squared symbol. The inset shows the MCT prediction for the same square well system, calculated using as input of the MCT the PY structure factor. Redrawn from [165], with APS permission.

for the attractive glass case [143, 166]. However, qualitatively, the theoretical predictions of the reentrant regime, with an associated crossover to logarithmic singularity, and glass-to-glass transition are confirmed by the detailed molecular dynamics calculations.

4.4. Higher-order singularities

The significant agreement between experiments, simulations and theoretical MCT predictions has prompted researchers to test, via specific accurate simulations, the most striking and unusual predictions of the theory. Recently, simulations have been designed to study numerically both the glass-glass transition and the dynamics close to an A_4 singularity [142, 143, 167]. Both these numerical studies have been performed using the SW binary mixture model discussed above. An important prediction of the theory regards indeed the presence of a kinetic (as opposed to thermodynamic) glass-glass transition, which should take place in the glass phase on crossing a critical temperature. Heating a short-ranged attractive glass should produce a sudden variation of all dynamical features, without significant structural changes. For example, at the transition temperature, the value of the long-time limit of the density-density correlation function, the non-ergodicity factor f_k ,

should jump from the value characteristic of the short-ranged attractive glass to the significantly smaller value characteristic of the HS glass. The numerical work suggests that the ideal attractive glass line in short-ranged attractive colloids has to be considered, in full analogy with what has been found in the study of glass-forming molecular liquids [26], as a crossover line between a region where ideal-MCT predictions are extremely good (in agreement with the previous calculation in the fluid phase) and an activated-dynamics region, where ideal-MCT predictions apply in a limited time window. The anomalous dynamics, which stems from the presence of a higher-order singularity in the MCT equations [137, 138, 166], still affects the dynamical processes in the fluid and in the glass, even if activated processes pre-empt the possibility of fully observing the glass–glass transition phenomenon, at least in the SW case [168]. It is important to note that systems in which the short-ranged inter-particle potential has a shape enhancing the bond lifetime, could produce dynamics which are less affected by hopping processes, favoring the observation of the glass–glass phenomenon.

Simulations have also been performed to investigate the dynamics close to the A_4 point [166]. In the SW case, the systems are characterized by three control parameters, the packing fraction ϕ , the ratio of the thermal energy to the typical well depth u_0 and the range Δ of the attractive potential. Within MCT, the phase diagram of this three-dimensional control parameter space is organized around a critical point (T_4, ϕ_4, Δ_4) , referred to as a type A_4 higher-order glass transition singularity in the MCT classification. A_4 is the end point of a line of higher-order singularities (of type A_3). From a physical point of view, A_4 is characterized for being the simplest higher-order singularity on a type B transition line accessible from the liquid phase. For $\Delta > \Delta_4$ no singular points are predicted by the theory, while for $\Delta < \Delta_4$ the A_3 singularity points are buried in the glass phase, and their presence can be observed only indirectly. Near the A_4 singularity, MCT predicts a structural relaxation dynamics, which is utterly different from that known for conventional glass-forming liquids. It is ruled by logarithmic variations of correlators as a function of time and sub-diffusive increase of the mean squared displacement. Theory makes precise predictions for the time interval where this unusual dynamics is expected, as well as for its variation with changes of the T , Δ and ϕ control parameters. The simulation data – with parameters explicitly chosen close to the A_4 point – exhibit the mentioned laws over time intervals up to four orders of magnitude, as shown in figure 13. More importantly, the decay patterns vary with changes of the control parameters and wavevectors as expected [142, 169], properly testing the theoretical predictions.

4.5. Mechanical properties

The dynamic differences between the attractive and repulsive glasses discussed above generate differences in the mechanical properties of the two glasses. In general terms, glasses dominated by attraction have a stronger rigidity under shear than those produced simply by packing forces. This phenomenon originates from the changes in the non-ergodicity factor associated to the glass–glass transition, which lead the system to soften with respect to shear on approaching the repulsive glass. New possibilities are expected to arise from further studies of the mechanical properties

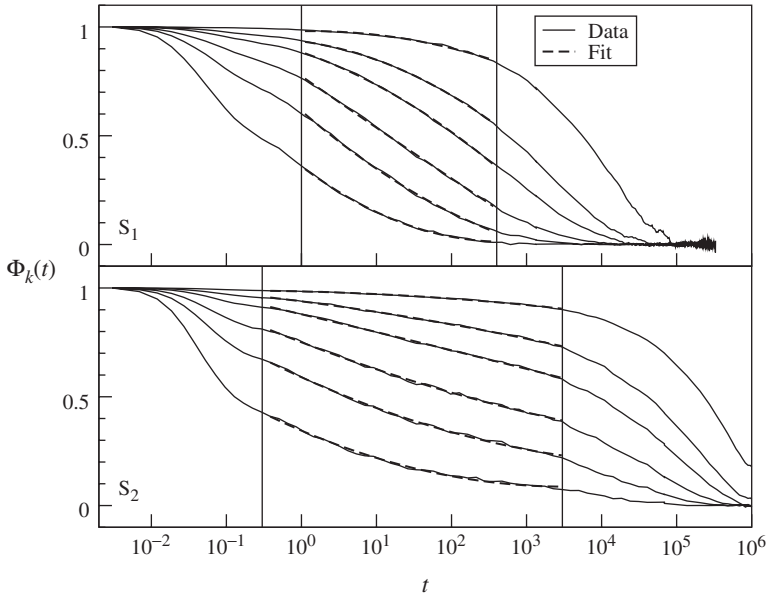


Figure 13. *Decay of the density fluctuations close to a higher-order singularity.* Numerical study of the density fluctuation correlators in a 50–50 binary mixture of particles of size ratio $\sigma_{BB}/\sigma_{AA} = 1.2$ at $T/u_0 = 0.4$ and $\phi = 0.6075$ for two different values of the well width, close to the estimated position of the A_4 singularity of the SW ($T/u_0 = 0.416$; $\Delta_{ij} = 0.043\sigma_{ij}$; $\phi = 0.6075$). Six different wave vectors (from top to bottom $k\sigma_{BB} = 6.7, 11.7, 16.8, 23.5, 33.5$ and 50.3) are shown. The long dashed lines are fits according to the MCT predictions for systems close to the A_4 singularity. The vertical dashed lines indicate the fitting interval. The top panel refer to the states S_1 (SW width 0.031 of the particles diameter) and the bottom panel to the state S_2 (width 0.043). Note that on approaching the A_4 singularity, the range of validity of the asymptotic MCT predictions increases by one order of magnitude in time. Note also the large window in which an essentially logarithmic decay in time is observed for a selected value of k . Redrawn from [166] with APS permission.

of short-range colloidal systems. The short-range bonding characteristic of the low temperature (attractive) glass produces a much stiffer material than the one formed at high temperature (repulsive glass). By tuning the volume fraction and the attraction range, it should also be possible to design a material where the transition between the attractive and repulsive glass takes place without any intermediate liquid phase, i.e. a glass-to-glass transition. In these specific conditions, a small change in the external parameters would produce a remarkable change in the elastic properties of the material with no significant structural change. Theoretically, more than one order of magnitude change in the stiffness is expected. For material scientists, design production and technological exploitation of such a material is one of the most fascinating challenges opened by the study of the dynamic properties of short-range attractive colloids. In this respect, MCT calculations, whose predictive power has been significantly strengthened by the close agreement between predictions and experimental observation, might become a valuable instrument for guiding the design of novel soft materials with specific properties.

The theoretical predictions of the viscoelastic behavior of the fluid phase, close to dynamic arrest, is receiving significant attention in the last years [53, 171–174]. The richness of the dynamics in the short-range attractive colloids can provide a valuable test case for comparing theoretical predictions and numerical data. Viscoelastic properties of the Asakura–Oosawa and SW models have been recently studied numerically, computing the shear viscosity η as the integral of the correlation function of the non-diagonal terms of the microscopic stress tensor,

$$\sigma^{\alpha\beta} = \sum_{i=1}^N m v_{i\alpha} v_{i\beta} - \sum_{i<j}^N \frac{r_{ij\alpha} r_{ij\beta}}{r_{ij}} V'(r_{ij})$$

where $v_{i\alpha}$ is the α -th component of the velocity of particle i , and V' is the derivative of the total potential. More precisely

$$\eta \equiv \int_0^\infty dt C_{\sigma\sigma}(t) = \frac{\beta}{3V} \int_0^\infty dt \sum_{\alpha<\beta} \langle \sigma^{\alpha\beta}(t) \sigma^{\alpha\beta}(0) \rangle, \quad (2)$$

where V is the volume of the simulation box. It has been found that η diverges following a power law as the transition points (attractive and repulsive) are approached, with the same exponent as the time scale of the density fluctuations, but different from that of the self diffusion [175]. On approaching the glass transition, the slow-decaying part of the $C_{\sigma\sigma}(t)$ can be time rescaled into a master function which has the same shape as the square of the density–density correlation function at a specific wavevector k . For the case of the repulsive glass the inverse k value corresponds to the nearest neighbor distance, while in the case of the attractive glass it corresponds to distances comparable to the (short) range of attraction. This interesting feature can be related, within MCT, to the fact that $C_{\sigma\sigma}(t)$ can be expressed as [13, 176]

$$C_{\sigma\sigma}(t) = \frac{k_B T}{60\pi^2} \int_0^\infty dk k^4 \left[\frac{d \ln S_k}{dk} \Phi_k(t) \right]^2.$$

A particularly interesting calculation of the elastic shear modulus G' was performed in the region where the attractive glass line extends into the glass regions, separating two different types of glass, the repulsive and the attractive one, and ending in the higher-order singularity A_3 [170]. Figure 14 shows the discontinuity in G' when crossing the glass line, a signal of the difference between the two types of glass. The discontinuity tends to disappear on approaching the singularity A_3 .

4.6. Remarks on attractive colloids

Dynamical heterogeneities in a colloidal fluid close to the attractive glass line have been studied by means of computer simulations [177, 178]. A clear distinction between some fast particles and the rest, the slow ones, was observed, yielding a picture of the attractive glass composed of two populations with different mobilities. Analyzing the statics and dynamics of both sets of particles, it was shown that the slow ones form a network of stuck particles, whereas the fast ones are able to move over long distances. No string-like motion was observed for the fast

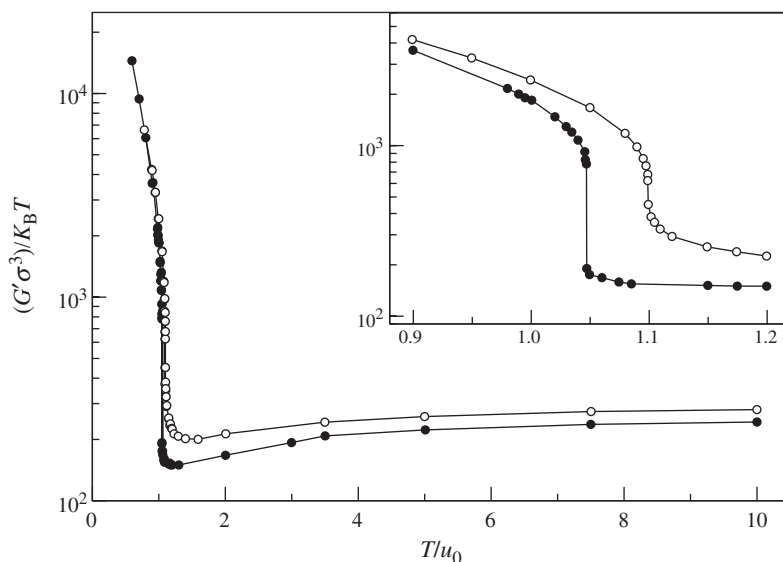


Figure 14. Behavior of the elastic shear modulus across the glass–glass transition region. Mode coupling predictions for the T -dependence of the elastic shear modulus G' for a short-range SW system with range of interaction equal to 0.031 of the hard core σ . $\phi = 0.5397$ (full circles) and $\phi = 0.5441$ (empty circles). The lines are a guide to the eye. The first ϕ value corresponding to crossing the glass–glass coexistence line. At this ϕ value a discontinuous change in G' is observed. The second corresponds to crossing the glass–glass line close to the endpoint A_3 . Here the width of the jump in G' approaches zero. Note also that G' in the attractive glass can be almost two orders of magnitude larger than the repulsive one. The inset shows a magnification of the transition region. Redrawn from [170] with APS permission.

particles, but they occupy preferential sites in the surface of the structure formed by the slow ones.

To conclude this section, we note the interesting possibility that the attractive glass line extends to low packing fraction acting as a gel line, an idea which would provide a unifying interpretation of the gel and glass arrested states of matter [139]. This idea has indeed been used to interpret experimental data on gelation in colloid-polymer mixtures [179, 180], postulating that the attractive glass line pre-empts the colloid-poor–colloid-rich phase separation process, which is expected to take place at low packing fractions. Recent simulations have addressed specifically this issue, for the binary SW case, attempting to locate the actual dynamic arrest lines in the full thermodynamic phase diagram of the system. The results of the numerical calculations show unambiguously that in the SW case, arrests at low packing fraction results from an interrupted colloid-poor–colloid-rich phase separation, caused by the glass transition which takes place in the dense regions created during the spinodal decomposition kinetics after a deep quench [181–185]. The fundamental reasons for gel formation in colloidal systems [186] and the possible routes to gelation are one of the topics which clearly requires additional work.

As a final remark, on theoretical and simulation studies, bases on effective one-component potentials, we point out that, while, in principle, the structural properties

of the colloidal particles can be reproduced by a proper effective one-component potential [147], there is no guarantee that dynamic properties in the original and in the effective one-component system are similar [187]. In the case where attraction is induced via addition of a small second component, the relative short-time mobility of the constituent components may play a crucial role in determining the occurrence of vitrification of a fluid or melting of a glass. Recent numerical results [188] suggest that a reentrant glass scenario requires not only a large size asymmetry but also that the short-time mobility of the added component be much higher than that of the glass-forming species. It has been found that if the short-time mobilities of the two species are comparable, the depletion potential still exactly determines the partial static structure of the larger component, but not its dynamical behavior. More work in this direction is expected in the next years.

5. Soft colloids

5.1. Charged colloids and the Wigner glass

Charge and sterically stabilized colloidal particles have been extensively studied as ideal model systems, since they are much more suitable than molecular systems to investigate the static and dynamic properties of strongly interacting particles, with particular emphasis on phenomena like melting, crystallization and glass transition. While uncharged colloids are mostly interpreted in terms of HS systems, charged ones are mostly modeled using screened Coulomb interactions. In dilute systems the potential is essentially soft, while in dense systems both the short-range hard core and the long-range repulsion play an important role.

In the simpler case, the system is composed of spherical charged mesoscopic particles, the macroions, immersed in a solvent. Both counterions and co-ions present in the solvent screen the colloid–colloid Coulomb interactions. The general electrostatic problem can be treated at various level of approximations, using the Poisson–Boltzmann equation or the Debye–Hückel approach, where ions are considered point-like and the equations are linearized. The effective inter-colloid interactions can then be modeled with a screened Coulomb potential which can be written as a hard core interaction complemented by a Yukawa repulsive potential. The Yukawa potential is defined as

$$V_Y(r) = A \frac{e^{-r/\xi}}{r/\xi}. \quad (3)$$

where A is a strength parameter and ξ a measure of the Debye screening length, which is determined by the concentration of counterions and co-ions, the latter when electrolytes are present. We note that, for the Yukawa potential, it is possible to derive an analytic solution of the Ornstein–Zernike equation for the direct correlation function in the mean spherical approximation [189]. Within the linearized Poisson–Boltzmann equation

$$A \equiv \frac{Z^2 e^2}{4\pi\epsilon\epsilon_0(1 + \kappa\sigma/2)} e^{\kappa\sigma} \quad (4)$$

and

$$\kappa^2 \equiv 1/\xi^2 = \frac{1}{\epsilon\epsilon_0 k_B T} \left(Ze^2 n_c + \sum_i z_i^2 n_i \right). \quad (5)$$

Here Z is the effective charge of the macroions, e is the electron charge, ϵ_0 is the vacuum dielectric constant, ϵ the solvent relative dielectric constant, n_c the colloid number density and z_i and n_i the valence and the number density of the i -th co-ion.

It is important to stress that the assumption of linear response is strictly valid only for dilute suspensions of weakly charged macroions. The range of validity of the linear response approximation on increasing colloid concentration or on high Coulomb coupling, especially in the presence of multivalent counterions, is still an open question [190]. *Ab initio* calculations suggest [191] that the general form of the screened Coulomb pair potential at appreciable concentrations remains valid, although with renormalized parameters. We also note that within the electrostatic calculation, the possibility of a state dependence of the effective colloid charge, driven by specific interactions with counterions and salts is neglected. It also appears that the hypothesis of pair-wise additive interaction starts to break down when the colloid concentration is such that more than two particles are found simultaneously within a distance smaller than the screening length [192, 193]. Finally, we note that the definition of ion number density should be based on the volume accessible to the ions [194].

Charged colloids crystals [195], when particles are interacting essentially with repulsive Coulomb interactions, could be considered the classical analogue of the Wigner crystals predicted for electrons [196, 197]. Due to the long-range of the repulsive interactions, the inter-particle distances in the crystal are much larger than the size of the particles, leading to ordered solid phases of low density compared to normal crystals. For these reasons, the phase diagram of the Yukawa repulsive potential (equation 3) has been extensively studied through experiments [198], theory [199–205] and numerical simulation [206–208] over a wide density range.

The phase diagram of the Yukawa potential shows a liquid phase at low density, followed by a *bcc* crystal phase and a *fcc* crystal. Since the potential is a function of r/ξ , the phase diagram for arbitrary ξ values can be scaled by using the dimensionless quantity

$$\lambda = n^{-1/3} \xi^{-1} \quad (6)$$

with n the number density. The variable λ is a measure of the average interparticle distance in units of ξ . Possible choices of dimensionless temperature T^* include $T^* \equiv k_B T/A$ or

$$T^* \equiv \frac{k_B T}{V_Y(\lambda\xi)} = \frac{k_B T \lambda}{A e^{-\lambda}} \quad (7)$$

where the thermal energy $k_B T$ is scaled by the potential energy evaluated at $\lambda\xi$. Figure 15 reports the phase diagram of the repulsive Yukawa potential based on extensive numerical simulations. In [206, 207], the freezing transitions between liquid phase and *bcc* and liquid and *fcc* crystals were calculated from the simulations by using the Lindemann and Hansen-Verlet criteria for melting. The numerical results

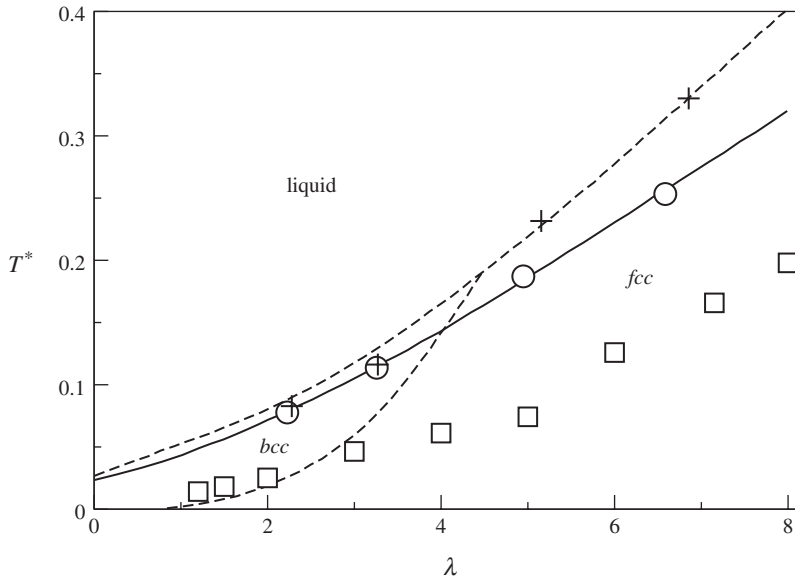


Figure 15. *Phase diagram of the Yukawa potential.* The average particle distance λ and the scaled temperature T^* are defined in equations 6 and 7 respectively. The circles indicate the coexistence points calculated numerically. The solid line is the estimate for the melting line. The pluses refer to the solid states with Lindemann-criterion ratio equal = 0.19. The dashed lines indicate the phase diagram calculated in [206, 207]. The squares are the glass transition points calculated with ideal MCT [209] using as input the structure factor calculated from molecular dynamics trajectories. Redrawn from [208]. Courtesy of the authors, with American Institute of Physics publications (AIP) permission.

showed agreement with the experiments, and pointed in favor of the accuracy of the Lindemann criterion with a mean squared displacement equal to 0.19 of the average particles distance, for small inter-particle distances. Later on, Meijer and Frenkel [208] performed a more accurate simulation of the Yukawa system and computed the free energies of the liquid and the solid phases, obtaining a Lindemann ratio of 0.19 for the *bcc*-liquid transition, and of 0.16 for the *fcc*-liquid melting. As shown in Meijer and Frankel [208], the coexistence region between fluid and crystal is extremely small.

Lindsay and coworkers [195] used monodisperse colloidal crystals and measured the shear moduli which are related to the energy density and therefore to the inter-particle potential. The crystals are characterized by Bragg scattering and shear rigidity, evidenced by a finite shear modulus and interpreted as the analog of the classical Wigner crystals, as mentioned above. Analogous measurements in binary systems of similar colloids gave instead rise to Wigner glasses, showing rigidity but no Bragg scattering. Sirota and coworkers [198] later performed a synchrotron X-ray scattering study of the complete phase diagram of polystyrene spheres (polyballs) and found a qualitative agreement with the theoretical predictions on charged colloidal systems, at least for small volume fractions (below 20%) of the colloid. Criteria for melting and freezing also seemed to be verified. A glass phase was obtained at a volume fraction of 20%, somewhat unexpected in a one-component system.

Turning more specifically to the liquid–glass transition, we recall that, once the structure factor is known, the MCT equations can be solved numerically for the Yukawa potential, and from the calculation of the asymptotic value of the density correlators it is possible to calculate the line of liquid to glass transition. This study has been performed by Lai *et al.* in particular for charged colloidal dispersions, using a HS potential followed by a Yukawa repulsive interaction [210]. A subsequent careful analysis [211] of the approximations has been used to introduce a rescaling of the static structure factor, necessary in order to avoid unphysical values of the system parameters. The rescaling has been employed to calculate the ergodic to non-ergodic transition in the same system for very high density colloids in a more reliable way. More recently a detailed analysis of the glass transition in pure Yukawa systems (i.e. point-like macroions without hard core short-range repulsion) has been performed by numerical simulation and through the solution of MCT equations [209]. The exact structure factor, obtained numerically, was used in order to calculate the liquid–glass transition line that is reproduced in figure 15. The shape of the theoretical glass line in the temperature–density plane has been found to be very similar to the shape of the isodiffusivity lines. As it is often the case, the glass line follows the same general pattern and shows a behavior very close to the one of the melting line. It is worth observing that, in simulations of the one-component Yukawa system, crystallization always prevents the possibility of equilibrating metastable states, in which a clear caging phenomenon is observed in the dynamic properties. While in the HS case the introduction of a small polydispersity appears to significantly slow down crystallization, thus offering the possibility of studying on the computer time scale slow dynamics processes, in the Yukawa case comparable polydispersity in ξ or A is not sufficient to prevent crystallization.

Further experimental evidence for Wigner glasses has been provided by Härtl *et al.* [212] and Beck *et al.* [213]. Static and dynamic light scattering in concentrated suspensions of spherical charged polymer colloids showed an amorphous phase for volume fractions larger than 0.22. Static scattering experiments furnished structure factors very similar to the HS systems (with the appropriate re-definition of the length scale). The dynamic scattering gave correlation functions that showed the typical plateau characteristic of a glass phase. The experimental results were compared with the general predictions of MCT. In particular dynamic correlators have been successfully interpreted in terms of the MCT β -correlator and the von Schweidler power law.

An example of Wigner glass could be provided by the arrested states observed in Laponite colloidal suspensions in the absence of added salt [214], although alternative interpretations have been given, ranging from frustrated nematic transition, micro-segregation and gelation [215]. Laponite is a synthetic clay made of disc-like colloidal particles with a diameter of ≈ 30 nm, a height of 1 nm, a charge of the order of a few hundreds and forms a suspension which is nearly monodisperse. Since the colloidal particles are charged, there is a long-ranged repulsive screened Coulomb potential of the Yukawa form to which a van der Waals short-ranged attraction, or an electric quadrupolar term, is to be added.

The hypothesis of a Wigner glass has been formulated in a series of papers where the authors [214, 216–218] have performed a study of a charged colloidal suspension,

focussing in particular on non-ergodic states of the system which is not in an equilibrium state. They have made a qualitative analysis of the suspension, making a distinction between gel and glass formation, related to the attractive and repulsive components of the interparticle potential. In particular, aging of a glass is related to the presence of cages of particles at high concentration due mainly to repulsive interactions, while gelation corresponds to cluster formation due to attraction. The study is made in terms of the ionic strength of the solution I , which is related to the Debye screening length ξ through $I = (2e^2/\epsilon k_B T \xi)^2$. The system reveals a different behavior below the value 10^{-4} and above 10^{-3} . Low values of $I < 10^{-4}$ are dominated by repulsive interactions of the Coulomb type and are interpreted as repulsive glassy states. At higher values $I > 10^{-3}$ gel states are found, connected to the attractive part of the potential. In the intermediate region the competing attractive and repulsive parts of the potential are effective and might give rise to an attractive glass. Finally at high values of $I > 10^{-2}$ phase separation occurs. The simultaneous existence in the state diagram of glassy and gel states opens the possibility of a liquid-to-solid transition when the system is ergodic.

Recently Ruzicka *et al.* [219] have performed an extended dynamic light scattering experiment on Laponite and have detected aging and structural arrest for both low and high concentrations, the dividing value being of the order 0.015–0.018 in weight concentration. Originally this value was supposed to be separating a stable liquid phase from a gelling system. Measurements performed over long periods of time have instead shown two different routes to gelation, related to the shape of the interatomic potential which contains attractive and repulsive parts. The situation is therefore reminiscent of the situation of competing interactions which gives rise to Wigner-type glasses [209]. Therefore, the low concentration phase is interpreted in terms of a cluster phase which produces a sort of fragile gel. The long times needed are due to the phase of formation of the clusters. The high concentration Laponite colloid is again interpreted as a Wigner glass, composed now of Laponite platelets, due to the fact that the effective packing fraction of the suspension is of the order of 0.43 because of the Debye-Hückel sphere associated with each platelet. As a concluding remark we may suggest that the clay platelets of Laponite seem to possess many of the features that are expected from a Wigner glass.

A different interpretation was proposed by Nicolai and coworkers [215, 220, 221] based on a picture in which aggregation between the platelets is induced by salt addition, which reduces electrostatic repulsion and produces fractal aggregates that will eventually form a gel. It was suggested that attractive interaction leads to aggregation of the Laponite particles and the formation of a *house of cards* structure. To support the proposed picture, it was recently shown that the presence of positive charges on the rim of the Laponite disks is necessary to induce aggregation and gelation [215]. These charges were neutralized by added pyrophosphate and aggregation and gelation was slowed down, even though the resulting ionic strength was increased. A revised state diagram was recently proposed in which a distinction between homogeneous and inhomogeneous dispersions was made and where it was argued that the sol–gel distinction is largely arbitrary. Simulations of simple models of Laponite [222–224] may help resolving this controversy.

5.2. Competing interactions: cluster phases

In several colloidal systems, as in the case of Laponite discussed above, the excluded volume and the screened electrostatic interactions are complemented by an attractive component, which can have quite different physical origins. The classical example goes back to the celebrated Derjaguin, Landau, Verwey and Overbeek (DLVO) [225] form of the interparticle potential, which has contributions from the hard core of the particles, the screened Coulomb electrostatic interaction and the dipolar van der Waals attraction. The final form of the potential depends parametrically on various physical quantities relating to the state of the colloidal dispersion, e.g. the charge and concentration of the counterions, the co-ions and the temperature. Quite often, the range of the attractive interaction is significantly smaller than the range of the repulsive electrostatic interaction. In these cases, the competition between the two length scales gives rise to a wide variety of phenomena. We consider in more detail cluster phases in equilibrium, as a possible path to spontaneous pattern formation in kinetically arrested states.

Equilibrium cluster formation was observed by Segrè and coworkers [226] in a colloidal sample of PMMA particles (mean radius $a = 212$ nm) where the addition of polystyrene induces an attractive depletion interaction. The main aim of the experiment, static and dynamic light scattering, was to investigate the similarities between the glass transition and the arrest at low packing fraction. Static measurements, reproduced in figure 16, showed the presence of a low- k peak in the structure factor

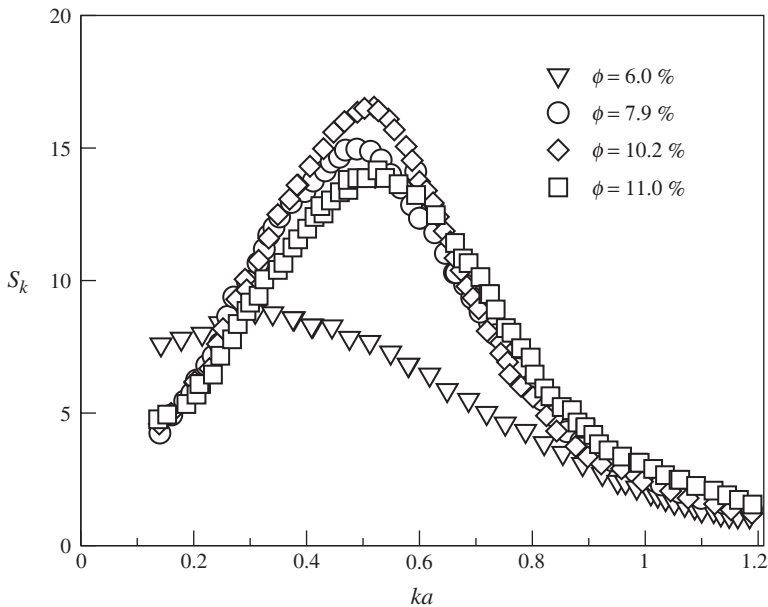


Figure 16. *Static light scattering in a cluster phase colloidal system.* The figure shows the static structure factor S_k at four different PMMA volume fractions, listed in the figure. All samples are fluid-like, except the one at $\phi = 11.0\%$ which behaves as an elastic solid. Note that the peak position is smaller than the position of the nearest neighbor peak, located around $ka = \pi$. Redrawn from [226], courtesy of the authors, with APS permission.

S_k which evolves towards small k and reaches a situation of kinetic arrest at $k_c a \approx 0.5$, where it remains essentially unchanged. The peak is attributed to the formation of fractal clusters of fractal dimension d_f . The value of k corresponding to the cluster peak turns out to give rise to a characteristic length ξ of the order of $\xi \approx \pi/k \approx 6a$, which gives an estimate of the cluster size and their average spacing. The cluster volume fraction is then $\phi_c = \phi(\xi/a)^{3-d_f}$ and gelation occurs when $\phi_c \approx 1$ which gives $\xi \approx a\phi^{-1/(3-d_f)}$ and a momentum transfer $ka \approx \pi a/\xi = \pi\phi^{-1/(3-d_f)}$, which in the measured case, $\phi = 0.11$ with $d_f = 1.8$, predicts the correct value $ka \approx 0.5$ for the structure factor peak. The proposed physical interpretation of the phenomenon is that dynamical arrest occurs when clusters touch because of the high volume fraction, leading to a non-ergodicity transition. Turning to dynamical behavior, the intermediate scattering function, probed by light scattering, exhibits the typical two-step decay characteristic of the glass transition. This effect is somewhat hard to observe due to the fact that clusters are rather fragile, and their bonds can be easily broken under the effect of gravity. Density matching of the dispersed phase and the solvent was necessary in order to observe ergodicity breaking. The previous conclusions have been tested in an imaging experiment, performed by the same group [227], using confocal microscopy in the same systems. The investigation focussed in the study of the bond formation among the PMMA particles which leads to dynamic arrest. The sample preparation implies the existence of a charge on the particles which results in a long-range repulsion, an important ingredient in the explanation of the kinetics of formation of cluster phases.

The possibility of formation in equilibrium of large clusters of colloidal particles was first proposed by Grönwold and Kegel [228]. They suggested a mechanism of aggregation, based on the effect of a short-range attraction combined with the stabilizing effect of small charges on the particles, which provided the long-range repulsive interaction, preventing eventually large-scale phase separation. The same authors have also made an interesting parallel with the effects in nuclear matter due to the simultaneous presence of short-ranged attractive and long-ranged repulsive forces [229]. A partial test of these predictions was made in an experiment of Sedgwick and coworkers [230] on a colloidal system (PMMA) with depletion interactions and residual charges on the particles. A cluster phase in coexistence with monomers, followed by dynamic arrest was observed, some aspects of which were in agreement with the model of Grönwold and Kegel. The small size of the clusters, together with the lack of a dynamic equilibrium between clusters and monomers, led the authors to conclude that the mechanism of aggregation was still unclear.

Equilibrium cluster phases have also been studied in numerical simulations [209]. The principal aim was to investigate the interplay between gel formation and glass formation as manifestations of a more general kinetic arrest phenomenon. The used interparticle potential is composed by a long-range Yukawa repulsive interaction (equation 3) and by a short-range potential V_{SR} of the form proposed by Vliegthart and coworkers [231], which is a generalization of the Lennard-Jones potential, and that mimics a hard core followed by an attractive well

$$V_{SR} = 4\epsilon \left[\left(\frac{\sigma}{r} \right)^{2\alpha} - \left(\frac{\sigma}{r} \right)^\alpha \right]$$

with $\alpha = 100$. The numerical study confirmed the possibility of generating both equilibrium cluster phases and kinetically arrested phases, and identified the structural signature in the low k pre-peak of the structure factor. The final state results from a subtle competition between aggregation (triggered by T) and repulsion. In [209] dynamic arrest was interpreted as a Wigner glass transition of the clusters fluid. Indeed, under the hypothesis of spherical homogeneous clusters of radius R , the cluster–cluster interaction is found to be of Yukawa form, with the same screening length ξ as in the monomer–monomer interaction, but with renormalized amplitude given by the expression

$$A(R) = A \left\{ 2\pi\xi^3 n e^{-R/\xi} \left[1 + \frac{R}{\xi} + \left(\frac{R}{\xi} - 1 \right) e^{2R/\xi} \right] \right\}^2$$

where n is an effective monomer number density in the cluster. Following a T -jump, the aggregation process can be thus visualized as a flow on the Yukawa phase diagram, due to the simultaneous change of the cluster number density and T^* (equation 7). If the melting or the glass lines of the Yukawa model are crossed during the cluster growth, the system becomes solid, i.e. a cluster crystal or, due to polydispersity of the aggregates, a cluster glass. Similar models have been studied by Coniglio and coworkers [232], using an interaction which mimics the DLVO potential, with a finite value at contact.

Equilibrium cluster formation has been experimentally observed also in concentrated protein solutions and colloids by Stradner *et al.* [233]. The experiments have been performed on lysozyme by small-angle X-ray and neutron scattering, with in mind the typical application of protein crystallization, i.e. the ability to form high quality crystal. They also used spherical colloidal particles interacting with a short-range attraction, induced by depletion effects, and with a long-range repulsion, due to a small residual charge on the colloids. In these cases too two peaks are observed in the structure factor as a function of momentum transfer: the one at low values is related to cluster–cluster correlations and is concentration independent but temperature dependent, the second one is due to monomer–monomer correlations within the dense clusters and is both concentration and temperature independent (figure 17). Therefore, the data are interpreted in terms of self-assembling of particles into small clusters due to the short-range attraction, and limitation of the growth due to long-range repulsion.

Baglioni *et al.* [234] have performed a detailed experimental study of concentrated protein solutions (cytochrome C protein) using small-angle neutron scattering (SANS) and viscosity measurements. They observed intensity spectra that can be described by screened Coulomb Yukawa-type interactions first, but require attractive interactions upon increase of the pH of the dispersion. When salt is added to the protein solution, two peaks are detected in the SANS spectra and interpreted as due both to the usual protein–protein interaction and to cluster–cluster interaction at lower values of the wave vector k_c . The value of k_c is related to the average cluster size R_{max} by the simple relation $k_c = \alpha\pi/R_{max}$, where α is a constant of the order unity. The average cluster size is in turn simply related to the volume fraction ϕ by the power law giving fractal dimension of the aggregates $R_{max} = R_0 \phi^{1/(d_f-3)}$, with $R_0 = 16.3 \text{ \AA}$ the protein radius. A plot of $\ln[\pi/(k_c R_0)]$ as

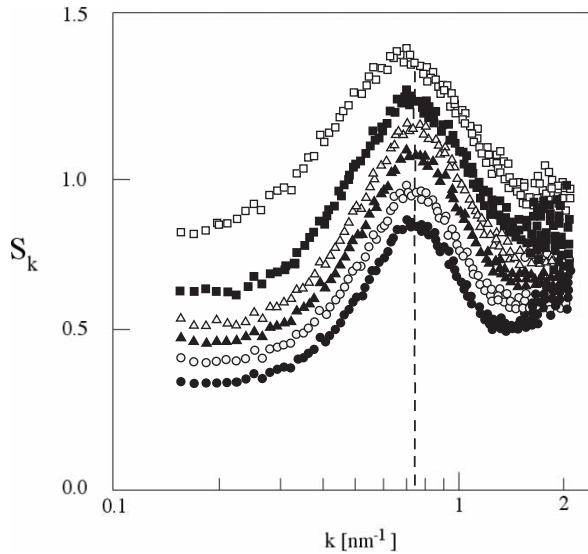


Figure 17. X-ray scattering intensity from a lysozyme solution. Structure factor obtained by small-angle X-ray scattering from lysozyme solutions (monomer radius 1.7 nm) of different concentrations ranging from 36 mg ml^{-1} (open squares) to 273 mg ml^{-1} (filled circles). The dashed line indicates the cluster peak position, roughly independent on concentration. In this sample, the monomer peak position is at $k = 2.24 \text{ nm}^{-1}$. Redrawn from [233], courtesy of the authors, with permission of *Nature Publishing Group*.

a function of $\ln(1/\phi)$ nicely confirms this simple estimate of the cluster size. These observations are accompanied by a strong increase in the relative viscosity, and are interpreted as due to metastable arrested states and a signature of the gelation process along the lines outlined above.

MCT has been recently [235] applied to a model system in which particles interact via short-range attractive and long-range repulsive Yukawa potentials, using the structure factor calculated from the mean-spherical approximation for the equilibrium properties. The glass–glass reentrance phenomenon in the attractive colloidal case is observed in the presence of the long-range repulsive barrier, which results in a situation similar to the attractive and repulsive glasses reported above. Competition between the short-range attraction and the long-range repulsion produces characteristic behavior of the structure factor and the non-ergodicity factor. A careful analysis gives rise to new regimes which appear in the attractive glass, and are tentatively associated with a cluster liquid (called static cluster glass) and heterogeneous structures (dynamic cluster glass). Crossover points separating the different glass states are also identified along the liquid–glass transition line between the liquid and the attractive glass.

The shape of the cluster as a function of the cluster size has been studied by Mossa and coworkers for systems of particles with competing interactions [236]. In particular the ratio of the screening length ξ to the cluster size R_{max} appears to play an important role. As long as ξ exceeds R_{max} the clusters retain the spherical shape, but become elongated in the opposite limit. A characteristic cluster shape has

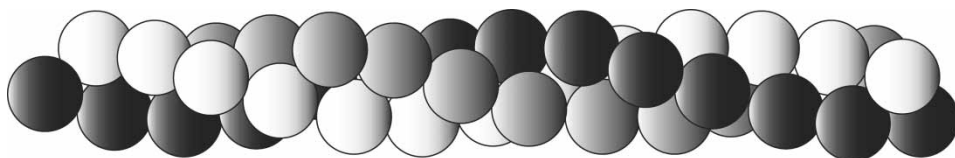


Figure 18. A pictorial view of the Bernal spiral. Particles have been shaded differently in order to highlight the presence of three strands. In the spiral each particle has exactly six neighbors.

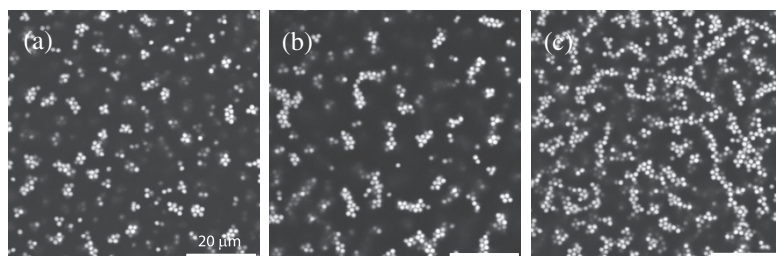


Figure 19. Confocal microscope images of colloid-polymer mixtures at different volume fractions. From left to right: $\phi = 0.080$, 0.094 , and 0.156 . The interparticle interaction is composed by a screened electrostatic repulsion and by a short-range depletion attraction. The attractive interaction is the same in all three samples. Images (a) and (b) show a cluster phase while (c) shows a network phase. Bars are $20\ \mu\text{m}$ long. Analysis of the coordinates shows that the gel is composed of branching Bernal spirals. From [239], courtesy of the authors, with APS permission.

been identified in the case of strong repulsive amplitude and short screening length, giving rise to a Bernal spiral [237], depicted in figure 18. The linear shape of the spiral can be reconstructed by considering it made by tetrahedra joined by a common face.

Quite recently an experiment performed by Campbell *et al.* on coated PMMA spheres, using three-dimensional fluorescence confocal microscopy [239], has evidenced in a clear way the existence of a cluster phase with the Bernal spiral shape, as shown in figure 19. In the experiment particles have a mean radius of $a = 777\ \text{nm}$, a 3% polydispersity, a mass density of $1.176\ \text{g cm}^{-3}$, a small positive charge of $140e$ and are both density and refractive index matched. The interactions are provided by a hard core of size $2a$, an attraction the range of which is measured by the radius of gyration $r_g/a \approx 0.12$ and a long-range Yukawa repulsion of range $\kappa a \approx 0.78$. What is observed is the presence of clusters at low volume fraction of the dispersed phase. When the latter increases the clusters form chains of particles which are identified as tetrahedra with a face in common. The final stage is a gel structure composed of Bernal spirals, as detected studying orientational correlations. Simulation of the same system, shown in figure 20 confirms the experimental picture [238]. See also [232].

The main ideas introduced in the description of cluster phases, in colloidal systems and in proteins, are strongly connected to the general work of pattern formation in the case of competing interactions of different range. Indeed these phenomena occur in a wide variety of systems, as for example water surfactant oil mixture [240], mixtures of block copolymers [241] and magnetic and dipolar fluids [242]. More recently, Sear *et al.* [243] have studied silver quantum dots at the

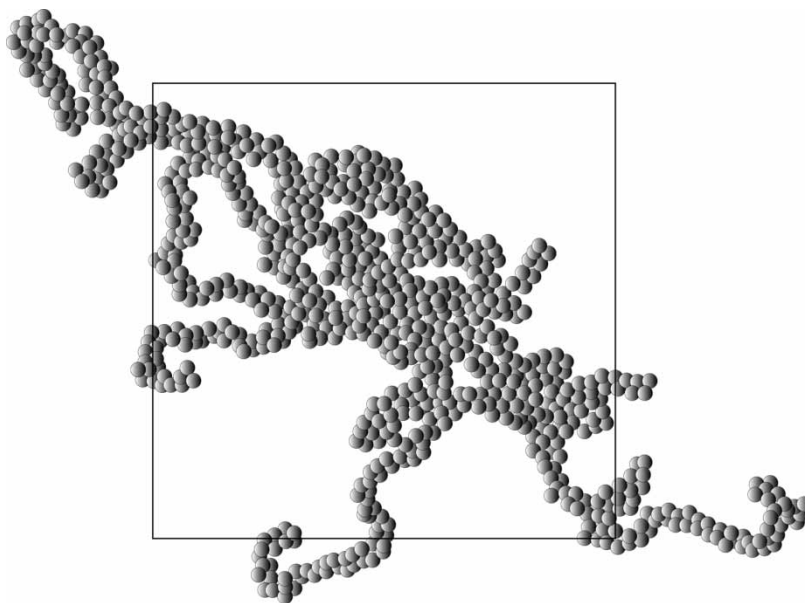


Figure 20. *Snapshot of a simulation of a Bernal spiral gel.* A pictorial description of the shape of the percolating cluster observed in a typical configuration at $\phi = 0.125$ for low temperature. The cluster spans, via periodic boundary conditions, the entire simulation box (full-line square). In the model, particles interact with a short-range potential complemented by a Yukawa repulsion. A close look to the figure shows that particles are locally tetrahedrally coordinated generating a one-dimensional arrangement of tetrahedra. The structure of the cluster is composed by large segments of Bernal spiral structures joined in branching points, the latter providing the mechanism for network formation.

water–air interface and confirmed the spontaneous formation of spatially modulated two-dimensional phases. When the concentration of the particles increases and the long-range repulsion becomes more important, the clusters formed by aggregation tend to pass from a spherical shape to stripelike arrays of dots. Two-dimensional spontaneous pattern formation and microphase separation was also observed in a recent computation of Imperio and Reatto [244] using Yukawa potentials.

An interesting system of interacting colloids and polymers where competing interactions play an important role, is made of an aqueous solution of linear and highly charged and flexible anionic polyelectrolytes, macromolecules carrying electric charges, and oppositely charged colloidal particles, cationic liposomes [245]. This system forms complexes, called lipoplexes, due to the adsorption of polyelectrolytes at the liposome surface. This process, which is rather complex, has been studied in detail and is responsible for the form of the interaction potential, with both short-range attraction and long-range screened repulsion. Two unusual phenomena are present in these type of systems: attraction between like charged particles and overcharging of the colloids. In this case, more counterions are adsorbed on the liposome surface than the ones necessary to neutralize the charge on the macroions, an effect that gives rise to a charge inversion, i.e. an overall charge of the macroion of opposite sign with respect to the original one. The adsorbed

polyions leave the macroion surface partially uncovered, since they tend to avoid each other in order to minimize electrostatic interactions. In other words, they form more or less ordered distributions of domains with excess negative charge, polyelectrolytes domains, and excess positive charge, polyelectrolyte-free domains. The inhomogeneous surface charge distribution gives rise to a short-range dipolar attraction between lipoplexes. As a consequence of the balance between the electrostatic repulsion and the charge patch attraction, the colloidal particles tend to aggregate and form large equilibrium clusters. In some cases the cluster phase seems to undergo a gelation process which shows aging. Transmission electron microscope images of cluster formation of liposomes of size ≈ 40 nm (dioleoyltrimethylammoniumpropane, DOTAP) due to the interactions with a polyelectrolyte (sodium polyacrylate salt, NaPAA) have clearly shown the formation of aggregates of increasing size, up to ≈ 400 nm [246]. A careful study [247] of the size distribution of the clusters shows also the reversible character of the lipoplex aggregation, and qualifies the clusters as equilibrium aggregates. As a final result, the analysis of the correlation functions obtained by dynamic light scattering in the aging regime show the presence of two correlation times. The longer correlation time increases with the waiting time, while the shorter one remains approximately constant. This behavior, typical of arrested systems, is attributed, according to the usual picture, to the fast motion of the particles in the cage formed by the neighbors in the cluster and to the slow process of escape from the cage. Although still at a semiquantitative level, these results fit in the general scenario of formation of an arrested phase due to competing interactions described earlier. The study of competitive interactions is in a quite active stage of development and has opened a large spectrum of applications in various fields of research on complex liquids.

5.3. *Ultrasoft colloids: star polymers*

Star polymers are systems which occupy an intermediate position between hard colloids with a strong repulsive core, such as HS, and soft flexible polymeric systems [147]. They are also called ultrasoft colloids. Star polymers are made of flexible arms, called functionality f , with one end linked to a common point. The number of arms varies from a few units to a rather large value; in the latter case the stars tend to behave as hard colloids, while lowering the functionality the interparticle potential becomes increasingly soft. Many interesting properties of star polymers have been clarified on the basis of an effective interaction potential between star polymer centers [248]. In line with their hybrid polymer–hard colloid character, star polymers display no crystallization transition when the functionality f is low, $f \leq 34$. At higher functionalities, a freezing transition takes place at about the overlap concentration of the system, into a *bcc* solid for lower functionalities and into an *fcc* solid for higher functionalities. The freezing is succeeded by either a re-entrant melting transition to the fluid for intermediate functionalities, $34 \leq f \leq 54$, or by a cascade of structural phase transitions at higher values of f . The functionality-dependent *bcc* and *fcc* solids, as well as the reentrant melting transition, have been experimentally observed in solutions of star-like block copolymer micelles. Though the crystalline solids are the phases of thermodynamic equilibrium at such high concentrations, the experimental situation is often somewhat different. A variety

of studies with star polymers or star-like systems of various functionalities has shown that it is quite difficult to nucleate a crystal. Especially at high functionalities, the solutions display a glass transition, i.e., a dynamical arrest into an amorphous crowded state in which the characteristic relaxation time of the system becomes extremely long [249–254]. The onset of arrest, as opposed to crystallization, is further enhanced by the presence of some polydispersity in the samples, which gets indeed more pronounced as functionality increases.

The analysis of star polymers is based on the effective center–center interaction potential

$$\begin{aligned}\beta V(r) &= \frac{5}{18} f^{3/2} \left[-\ln\left(\frac{r}{\sigma}\right) + \frac{1}{1 + \sqrt{f/2}} \right], & r \leq \sigma \\ &= \frac{5}{18} f^{3/2} \frac{\sigma/r}{1 + \sqrt{f/2}} \exp\left[-\frac{\sqrt{f}(r - \sigma)}{2\sigma} \right], & r \geq \sigma\end{aligned}$$

where r is the distance between the two centers. This potential is a combination of a logarithmic interaction at short distances, which gives the interaction its ultrasoft character and stems from the scaling analysis of Witten and Pincus [255], and a Yukawa form for the decay at long distances matched at a distance $r = \sigma$. The potential only depends on the length σ and the functionality f . The validity of this potential has been demonstrated via extensive comparisons both with SANS data [248, 252] and with monomer-resolved molecular dynamics simulations [256]. In this entropic effective potential f^{-1} plays the role of T in normal fluids.

Though the crystalline solids are the phases of thermodynamic equilibrium at high concentrations, the experimental situation is often somewhat different. To investigate arrest in star polymers, molecular and Brownian dynamics simulations have been performed for a large range of functionalities f and packing fractions ϕ . Simulations show that the dynamics of star polymer solutions is extremely rich. In order to approximate the line of structural arrest, the isodiffusivity curves have been evaluated. These lines display both minima and maxima as a function of ϕ and minima as a function of f , which then have been successfully connected to the behavior to the ϕ and f -dependence of the effective hard core diameter of an equivalent HS system. Even in this system, MCT provides an accurate modeling of the structural arrest in supercooled liquid states. The detailed comparison between theoretical predictions and simulation confirms that MCT is a valid approach for guiding the interpretation of the disordered arrested states of soft matter materials [144], offering a theoretical understanding for the observation of disordered arrested states not only in colloidal systems characterized by a hard core [7, 137, 138, 141, 152], or charge-stabilized colloidal dispersions [210, 211, 257, 258], but also in ultrasoft systems like star polymer solutions.

Recent works have addressed the issue of the effect of the addition of linear chains, or small star polymers, to a star polymer arrested state. It has been found [253] that the added polymer reduces the modulus of the gel, and in the limit of high polymer molecular weight or concentration, the gel melts. Within the liquified region, the reduced star viscosity drops upon further addition of linear polymer. The effective star linear polymer interactions are shown to be responsible for

the observed counterintuitive phenomena, via a depletion-like mechanism which explains the gel–liquid transition. Eventually, for very high molecular weights a reentrant gelation is observed and attributed to bridging flocculation induced by the long polymer chains. Thus, the addition of linear polymer chains to a multiarm star gel yields melting. Similar results were obtained when studying the influence of the addition of a component, with a small number of arms and a small size, on a concentrated solution of large stars with a high value of f [259]. Upon addition of the small ones, it was reported a loss of structure that can be attributed to a weakening of the repulsions between the large stars due to the presence of the small ones. These phenomena of melting upon addition offer unique opportunities to design and engineer novel nanostructured soft materials at the molecular level, leading to kinetic manipulation of the state of soft materials through additives, and achieving liquefaction or jamming. Moreover, they provide the framework for a thorough understanding and control of the interactions in soft matter physics, where macromolecular sizes and architecture critically influence the excluded volume, and thus, the entropic and kinetic character of phase transitions.

Finally, we note that block copolymer micelles have been recently used as model systems for investigating crystallization and kinetic arrest in ultrasoft star polymer systems [260, 261]. Indeed, micellar functionality f can be smoothly varied by changing solvent composition (interfacial tension). Structure factors obtained by SANS have been quantitatively described in terms of an effective potential for star polymers. The experimental phase diagram of star-like PEP–PEO block copolymer micelles [262] reproduces, to a high level of accuracy, the predicted liquid–solid transition. Interestingly enough, whereas for intermediate f a *bcc* phase is observed, for high f the formation of a *fcc* phase is preempted by glass formation.

6. Perspectives and conclusions

In the last years, a significant understanding of dynamic arrest in colloidal systems has been achieved, thanks to the close contact between experiments, simulations and theoretical studies. The present review aims at putting together a list of the relevant results, *albeit* incomplete. Still, the study of glassy dynamics in colloidal systems is far from being complete, and the present review will hopefully become quickly obsolete. Several reasons conspire in this direction. First, the incredible technical developments which are taking place in recent years and which provide experimental information with an unprecedented level of accuracy and detail [263]. Particles can now be followed in their actual trajectories, forcing a close comparison between experiments, simulations and theoretical predictions. The physical and chemical interactions between the particles (the effective interaction potentials) can also be accurately measured [264], providing a valuable input to theoretical work [192, 193]. Second, the ability to design and assemble new colloidal particles with specific shapes and interaction potentials will generate new classes of systems tailored for specific material properties [265]. In this respect, several new lines are developing to provide further control on the particle surface chemistry, control on the physical properties of the solvent, and more important shape control. We expect in the near future that colloidal particles of arbitrary shape can be produced, opening the way

to a revolution in colloidal physics, redesigning at colloidal level forms nowadays observed only in atomic and molecular fluids. Finally, it will be possible to control the properties of the materials using external fields, thanks to the possibility of embedding electric or magnetic dipoles within the colloids [266].

The possibility of fully exploiting these new challenges requires understanding not only the equilibrium phases of the system and their modifications with the external fields, but also understanding the kinetic phase diagram, i.e. the regions in phase space where disordered arrested states can be expected, and when and how these states are kinetically stabilized with respect to the ordered lowest free energy phases. In this respect, the study of the glassy dynamics plays an extremely relevant role. The concept of repulsive and attractive glass, of cluster phases, of reentrant glass melting will provide a framework for interpreting and developing new ideas in the study of tomorrow new materials. We also expect significant developments in understanding an aspect of slow dynamics and arrest in colloidal systems which we have not addressed in the present review. In particular we refer to the formation of colloidal gel states, arrested states at low packing fraction which can be formed both as a result of a colloid-poor–colloid-rich phase separation process, followed by a glass transition of the high packing fraction phase or, as expected when patchy colloids will become available, as equilibrium phase [267].

Finally, we cannot avoid noticing that, in most cases studied so far, MCT calculations provide a very consistent estimate of the location of the glass line and of its modification on changing the structure of the system. Even very peculiar features (as in the case of the dynamics close to higher-order singularities) have been predicted and successfully compared with experimental data. At present time, MCT is a valuable instrument for guiding the design of novel disordered soft materials with specific properties.

Acknowledgements

It is a pleasure to thank Wolfgang Göetze, Christos Likos and Emanuela Zaccarelli for carefully reading the manuscript and suggesting improvements to it. We acknowledge financial support from MIUR/COFIN, MIUR/FIRB and the Research and Training Network CRTN-CT-2003-504712 funded within the EU Marie Curie Program.

References

- [1] S.Z. Ren and C.M. Sorensen, *Phys. Rev. Lett.* **70** 1727 (1993).
- [2] F. Ikkai and M. Shibayama, *Phys. Rev. Lett.* **82** 4946 (1999).
- [3] S.K. Kumar and J.F. Douglas, *Phys. Rev. Lett.* **87** 188301-1 (2001).
- [4] J. Grandjean and A. Mourchid, *Europhys. Lett.* **65** 712 (2004).
- [5] G. Foffi, F. Sciortino, P. Tartaglia, E. Zaccarelli, F. Lo Verso, L. Reatto, K.A. Dawson and C.N. Likos, *Phys. Rev. Lett.* **90** 238301-1 (2003).
- [6] N.A.M. Verhaegh, D. Asnaghi, H.N.W. Lekkerkerker, M. Giglio and L. Cipelletti, *Phys. A* **242** 104 (1997).
- [7] K.N. Pham, A.M. Puertas, J. Bergenholtz, S.U. Egelhaaf, A. Moussaid, P.N. Pusey, A.B. Schofield, M.E. Cates, M. Fuchs and W.C.K. Poon, *Science* **296** 104 (2002).

- [8] S.H. Chen, W.R. Chen and F. Mallamace, *Science* **300** 619 (2003).
- [9] L. Cipelletti and L. Ramos, *J. Phys.: Condens. Matter* **17** R253 (2004).
- [10] V. Trappe and P. Sandkühler, *Curr. Opin. Colloid Interface Sci.* **8** 494 (2004).
- [11] K.A. Dawson, *Curr. Opin. Colloid Interface Sci.* **7** 218 (2002).
- [12] W.C.K. Poon, *Curr. Opin. Colloid Interface Sci.* **3** 593 (1998).
- [13] U. Bengtzelius, W. Götze and A. Sjölander, *J. Phys. C* **17** 5915 (1984).
- [14] W. Götze, in *Liquids, Freezing and Glass Transition*, edited by J.-P. Hansen, D. Levesque, J. Zinn-Justin (North Holland, Amsterdam, 1991), p. 287.
- [15] W. Götze and L. Sjögren, *Rep. Prog. Phys.* **55** 241 (1992).
- [16] W. Götze, *J. Phys.: Condens. Matter* **11** A1 (1999).
- [17] K. Kawasaki, *Trans. Theory Stat. Phys.* **24** 755 (1995).
- [18] E. Zaccarelli, G. Foffi, F. Sciortino, P. Tartaglia and K.A. Dawson, *Europhys. Lett.* **55** 157 (2001).
- [19] E. Zaccarelli, G. Foffi, P. De Gregorio, F. Sciortino, P. Tartaglia and K.A. Dawson, *J. Phys.: Condens. Matter* **14** 2413 (2002).
- [20] M.E. Cates, *cond-mat* **0211066** (2002).
- [21] T. Franosch, W. Götze, M.R. Mayr and A.P. Singh, *J. Non-Cryst. Solids* **235–237** 71 (1998).
- [22] T. Gleim, W. Kob and K. Binder, *Phys. Rev. Lett.* **81** 4404 (1998).
- [23] Th. Voigtmann, A.M. Puertas and M. Fuchs, *Phys. Rev. E* **70** 061506-1 (2004).
- [24] W. Götze and L. Sjögren, *Z. Phys. B* **65** 415 (1987).
- [25] S.P. Das, G.F. Mazenko, S. Ramaswamy and J.J. Toner, *Phys. Rev. Lett.* **54** 118 (1985).
- [26] S.P. Das and G.F. Mazenko, *Phys. Rev. A* **348** 2265 (1986).
- [27] S.P. Das, *Rev. Mod. Phys.* **76** 785 (2004).
- [28] U. Harbola and S.P. Das, *J. Stat. Phys.* **112** 1109 (2003).
- [29] W. Götze and Th. Voigtmann, *Phys. Rev. E* **67** 21502 (2003).
- [30] G. Szamel, *Phys. Rev. Lett.* **90** 228301-1 (2003).
- [31] G. Szamel, *Europhys. Lett.* **65** 498 (2004).
- [32] G. Szamel and E. Flenner, *Europhys. Lett.* **67** 779 (2004).
- [33] K.S. Schweizer and E.J. Saltzman, *J. Chem. Phys.* **119** 1181 (2003).
- [34] E.J. Saltzman and K.S. Schweizer, *J. Chem. Phys.* **119** 1197 (2003).
- [35] J. Wu and J. Cao, *Phys. Rev. Lett.* **95** 078301-1 (2005).
- [36] J. Horbach and W. Kob, *Phys. Rev. E* **64** 041503-1 (2001).
- [37] F. Sciortino and W. Kob, *Phys. Rev. Lett.* **86** 648 (2001).
- [38] J. Baschnagel and M. Fuchs, *J. Phys.: Condens. Matter* **7** 6771 (1995).
- [39] A. Brodin, M. Frank, S. Wiebel, G. Shen, J. Wuttke and H.Z. Cummins, *Phys. Rev. E* **65** 051503-1 (2002).
- [40] W. Götze and Th. Voigtmann, *Phys. Rev. E* **61** 4133 (2000).
- [41] D. Sherrington and S. Kirkpatrick, *Phys. Rev. Lett.* **75** 1792 (1975).
- [42] G. Parisi, *Phys. Rev. Lett.* **43** 1754 (1979).
- [43] M. Mezard and G. Parisi, *Phys. Rev. Lett.* **82** 747 (1999).
- [44] M. Mezard and G. Parisi, *J. Chem. Phys.* **111** 1076 (1999).
- [45] M. Cardenas, S. Franz and G. Parisi, *J. Chem. Phys.* **110** 1726 (1999).
- [46] B. Coluzzi, M. Mezard, G. Parisi and P. Verrocchio, *J. Chem. Phys.* **111** 9039 (1999).
- [47] F.H. Stillinger and T.A. Weber, *Science* **225** 983 (1984).
- [48] F. Sciortino, *J. Sta. Mech.* **P05015** (2005).
- [49] P.G. Debendetti and F.H. Stillinger, *Nature* **410** 259 (2001).
- [50] K. Kawasaki and K. Fuchizaki, *J. Non-Cryst. Solids* **235** 57 (1998).
- [51] D.S. Dean, *J. Phys. A* **29** L613 (1996).
- [52] K. Fuchizaki and K. Kawasaki, *J. Phys.: Condens. Matter* **14** 12203 (2002).
- [53] K. Miyazaki and D.R. Reichman, *Phys. Rev. E* **66** 050501 (2002).
- [54] S. Kirkpatrick, *Phys. Rev. B* **36** 8552 (1987).
- [55] T.R. Kirkpatrick, D. Thirumalai and P.G. Wolynes, *Phys. Rev. A* **40** 1045 (1989).
- [56] R. Richert, *J. Phys.: Condens. Matter* **14** R703 (2002).
- [57] J.P. Garrahan and D. Chandler, *Phys. Rev. Lett.* **89** 035704-1 (2002).
- [58] J.P. Garrahan and D. Chandler, *Proc. Natl. Acad. Sci.* **100** 9710 (2003).

- [59] M. Tokuyama and I. Oppenheim, Phys. Rev. E **50** R16 (1994).
- [60] M. Tokuyama and I. Oppenheim, Phys. A **216** 85 (1995).
- [61] M. Tokuyama, Phys. Rev. E **62** R5915 (2000).
- [62] M. Tokuyama, Phys. A **289** 57 (2001).
- [63] M. Tokuyama, H. Yamazaki and Y. Terada, Phys. Rev. E **67** 062403-1 (2003).
- [64] W. Kob and H.C. Andersen, Phys. Rev. E **48** 4364 (1993).
- [65] G. Biroli and M. Mezard, Phys. Rev. Lett. **88** 025501-1 (2002).
- [66] A. Lawlor, D. Reagan, G.D. McCullagh, P. De Gregorio, P. Tartaglia and K.A. Dawson, Phys. Rev. Lett. **89** 245503-1 (2000).
- [67] P. De Gregorio, A. Lawlor, P. Bradley and K.A. Dawson, Phys. Rev. Lett. **93** 025501-1 (2004).
- [68] P. De Gregorio, A. Lawlor, P. Bradley and K.A. Dawson, Proc. Natl. Acad. Sci. **102** 5669 (2005).
- [69] J.N. Israelachvili, in *Intermolecular and Surface Forces* (Academic Press, London, 1992).
- [70] G. Bryant, S.R. Williams, L. Qian, I.K. Snook, E. Perez and F. Pincet, Phys. Rev. E **66** 060501(R) (2002).
- [71] J.-P. Hansen and I. McDonald, in *Theory of Simple Liquids* (Academic Press, London, 1986).
- [72] B.J. Alder and T.E. Wainwright, J. Chem. Phys. **27** 1208 (1957).
- [73] S. Auer and D. Frenkel, Adv. Polym. Sci. **173** 149 (2005).
- [74] Z. Cheng, J. Zhu, W.B. Russel, W.V. Meyer and P.M. Chaikin, Appl. Opt. **40** 4146 (2001).
- [75] Z. Cheng, P.M. Chaikin, J. Zhu, W.B. Russel and W.V. Meyer, Phys. Rev. Lett. **88** 015501 (2002).
- [76] M. Sullivan, K. Zhao, C. Harrison, R.H. Austen, M. Megens, A. Hollingsworth, W.B. Russel, Z. Cheng, T. Mason and P.M. Chaikin, J. Phys.: Condens. Matter **15** S11 (2003).
- [77] P.N. Pusey and W. van Meegen, Nature **320** 340 (1986).
- [78] I. Volkov, J. Koplik and J.R. Banavar, Phys. Rev. E **66** 061401 (2002).
- [79] T.C. Hales, P. Sarnak and M.C. Pugh, Proc. Natl. Acad. Sci. **97** 12963 (2000).
- [80] S. Torquato, Nature **405** 521 (2000).
- [81] F.H. Stillinger and B.D. Lubachevsky, J. Stat. Phys. **73** 497 (1993).
- [82] A.S. Clarke and J.D. Wiley, Phys. Rev. B **35** 7350 (1987).
- [83] W. van Meegen, S.M. Underwood and P.N. Pusey, Phys. Rev. Lett. **67** 1586 (1991).
- [84] W. van Meegen and P.N. Pusey, Phys. Rev. A **43** 5429 (1991).
- [85] W. van Meegen and S.M. Underwood, Phys. Rev. Lett. **70** 2766 (1993).
- [86] S.I. Henderson, T.C. Mortensen, G.M. Underwood and W. van Meegen, Phys. A **233** 10290 (1996).
- [87] Th. Voigtmann, Phys. Rev. E **68** 051401-1 (2003).
- [88] W. van Meegen, Trans. Theory Stat. Phys. **24** 1017 (1995).
- [89] M. Fuchs, I. Hofacker and A. Latz, Phys. Rev. A **45** 898 (1992).
- [90] J.-L. Barrat, W. Götze and A. Latz, J. Phys.: Condens. Matter **1** 7163 (1989).
- [91] W. Götze and L. Sjögren, Phys. Rev. A **43** 5442 (1991).
- [92] L. Verlet and J.-J. Weis, Phys. Rev. A **5** 939 (1972).
- [93] G. Foffi, W. Götze, F. Sciortino, P. Tartaglia and Th. Voigtmann, Phys. Rev. E **69** 011505-1 (2004).
- [94] W. van Meegen, T.C. Mortensen, S.R. Williams and J. Müller, Phys. Rev. E **58** 6073 (1998).
- [95] M. Sperl, Phys. Rev. E (R) **71** 060401-1 (2005).
- [96] E.R. Weeks, J.C. Crocker, A.C. Levitt, A. Schofield and D.A. Weitz, Science **287** 627 (2000).
- [97] W.K. Kegel and A. van Blaaderen, Science **287** 290 (2000).
- [98] W. Kob, C. Donati, S.J. Plimpton, P.H. Poole and S.C. Glotzer, Phys. Rev. Lett. **79** 2827 (1997).
- [99] R.E. Courtland and E.R. Weeks, J. Phys.: Condens. Matter **15** S359 (2003).
- [100] U. Gasser, E.R. Weeks, A. Schofield, P.N. Pusey and D.A. Weitz, Science **292** 258 (2001).

- [101] R.J. Speedy, *Mol. Phys.* **95** 169 (1998).
- [102] L. Angelani, G. Foffi and F. Sciortino, *cond-mat* **0506447** (2005).
- [103] M. Cardenas, S. Franz and G. Parisi, *J. Phys. A* **31** 163 (1998).
- [104] G. Parisi and F. Zamponi, *cond-mat* **0506445** (2005).
- [105] T. Aste and A. Coniglio, *Europhys. Lett.* **67** 165 (2004).
- [106] J.N. Roux, J.-L. Barrat and J.-P. Hansen, *J. Phys.: Condens. Matter* **1** 7171 (1989).
- [107] S.R. Williams and W. van Meegen, *Phys. Rev. E* **64** 41502 (2001).
- [108] G. Foffi, W. Götze, F. Sciortino, P. Tartaglia and Th. Voigtmann, *Phys. Rev. Lett.* **91** 085701-1 (2003).
- [109] N.B. Simeonova and W.K. Kegel, *Phys. Rev. Lett.* **93** 035701-1 (2004).
- [110] L. Santen and W. Krauth, *Nature* **405** 550 (2000).
- [111] D. Frenkel, B.M. Mulder and J.P. McTague, *Phys. Rev. Lett.* **52** 287 (1984).
- [112] B. Groh and S. Dietrich, *Phys. Rev. E* **55** 2892 (1997).
- [113] M. Letz and A. Latz, *Phys. Rev. E* **60** 5865 (1999).
- [114] M. Letz, R. Schilling and A. Latz, *Phys. Rev. E* **62** 5173 (2000).
- [115] S.-H. Chong and M. Fuchs, *Phys. Rev. Lett.* **88** 185702 (2002).
- [116] S.-H. Chong and W. Götze, *Phys. Rev. E* **65** 041503-1 (2002).
- [117] S.-H. Chong, A.J. Moreno, F. Sciortino and W. Kob, *Phys. Rev. Lett.* **94** 215701 (2005).
- [118] A.J. Moreno, S.-H. Chong, W. Kob and F. Sciortino, *cond-mat* **0504744** (2005).
- [119] A. Donev, F.H. Stillinger, P.M. Chaikin and S. Torquato, *Phys. Rev. Lett.* **92** 255506 (2004).
- [120] S.R. Williams and A.P. Philipse, *Phys. Rev. E* **67** 051301 (2003).
- [121] A. Donev, I. Cisse, D. Sachs, E.A. Variano, F.H. Stillinger, R. Connelly, S. Torquato and P.M. Chaikin, *Science* **303** 990 (2004).
- [122] V.J. Anderson and H.N.V. Lekkerkerker, *Nature* **416** 811 (2002).
- [123] A.P. Gast, C.K. Hall and W.B. Russel, *J. Coll. Int. Sci.* **96** 251 (1983).
- [124] M. Baus and R. Achrayah, *J. Phys.: Condens. Matter* **47** 9633 (1996).
- [125] F. Fornasiero, J. Ulrich and J.M. Prausnitz, *Chem. Eng. Process* **38** 463 (1999).
- [126] L. Mederos, *J. Mol. Liq.* **76** 139 (1998).
- [127] H. Mahadevan and C.K. Hall, *AIChE J.* **36** 1517 (1990).
- [128] M.H.J. Hagen, E.J. Meijer, G.C.A.M. Moolj, D. Frenkel and H.N.W. Lekkerkerke, *Nature* **365** 425 (1993).
- [129] M.H.J. Hagen and D. Frenkel, *J. Chem. Phys.* **101** 4093 (1994).
- [130] M. Dijkstra, J.M. Brader and R. Evans, *J. Phys.: Condens. Matter* **11** 10079 (1999).
- [131] L. Mederos and G. Navascues, *J. Chem. Phys.* **101** 9841 (1994).
- [132] A. Vrij, M.H.G.M. Pend, P.W. Rouw, C.G. de Kruif, J.K.G. Dhont, C. Smits and H.N.W. Lekkerker, *Faraday Discuss.* **90** 31 (1990).
- [133] H. Mahadevan and C.K. Hall, *Fluid Phase Equilib.* **78** 297 (1992).
- [134] N. Asherie, A. Lomakin and G.B. Benedek, *Phys. Rev. Lett.* **77** 4832 (1996).
- [135] M. Dijkstra, *Phys. Rev. E* **66** 021402 (2002).
- [136] D. Fu, Y. Liu and J. Wu, *Phys. Rev. E* **68** 011403-1 (2003).
- [137] L. Fabbian, W. Götze, F. Sciortino, P. Tartaglia and F. Thiery, *Phys. Rev. E* **59** R1347 (1999).
- [138] L. Fabbian, W. Götze, F. Sciortino, P. Tartaglia and F. Thiery, *Phys. Rev. E* **60** 2430 (1999).
- [139] J. Bergenholtz and M. Fuchs, *Phys. Rev. E* **59** 5706 (1999).
- [140] R.J. Baxter, *J. Chem. Phys.* **49** 2770 (1968).
- [141] K.A. Dawson, G. Foffi, M. Fuchs, W. Götze, F. Sciortino, M. Sperl, P. Tartaglia, Th. Voigtmann and E. Zaccarelli, *Phys. Rev. E* **63** 011401-1 (2000).
- [142] M. Sperl, *Phys. Rev. E* **68** 031405-1 (2003).
- [143] M. Sperl, *Phys. Rev. E* **69** 011401-1 (2004).
- [144] F. Sciortino, *Nature Materials* **1** 145 (2002).
- [145] S. Asakura and F. Oosawa, *J. Chem. Phys.* **22** 1255 (1954).
- [146] R. Dickman, P. Attard and V. Simonian, *J. Chem. Phys.* **107** 205 (1997).
- [147] C.N. Likos, *Phys. Rep.* **348** 267 (2001).
- [148] W.C.K. Poon, *J. Phys.: Condens. Matter* **14** R859 (2002).

- [149] K.N. Pham, S.U. Egelhaaf, P.N. Pusey and W.C.K. Poon, *Phys. Rev. E* **69** 11503 (2004).
- [150] G. Foffi, E. Zaccarelli, S. Buldyrev, F. Sciortino and P. Tartaglia, *J. Chem. Phys.* **120** 8824 (2004).
- [151] F. Mallamace, P. Gambadauro, N. Micali, P. Tartaglia, C. Liao and S.H. Chen, *Phys. Rev. Lett.* **84** 5431 (2000).
- [152] T. Eckert and E. Bartsch, *Phys. Rev. Lett.* **89** 125701-1 (2002).
- [153] T. Eckert and E. Bartsch, *Faraday Discuss.* **123** 51 (2003).
- [154] T. Eckert and E. Bartsch, *J. Phys.: Condens. Matter* **16** S4937 (2004).
- [155] E. Bartsch, M. Antonietti, W. Shupp and H. Sillescu, *J. Chem. Phys.* **97** 3950 (1992).
- [156] E. Bartsch, V. Frenz, S. Mueller and H. Sillescu, *Phys. A* **201** 363 (1993).
- [157] E. Bartsch, *J. Non-Cryst. Solids* **192–193** 384 (1995).
- [158] E. Bartsch, V. Frenz, J. Baschnagel, W. Schaertl and H. Sillescu, *J. Chem. Phys.* **106** 3743 (1997).
- [159] D. Pontoni, T. Narayanan, J.-M. Petit, G. Gruebel and D. Beysens, *Phys. Rev. Lett.* **90** 188301-1 (2003).
- [160] D. Pontoni, S. Finet and T. Narayanan, *J. Chem. Phys.* **119** 6157 (2003).
- [161] W.R. Chen, F. Mallamace, C.J. Glinka, E. Fratini and S.H. Chen, *Phys. Rev. E* **68** 041402-1 (2003).
- [162] A.M. Puertas, M. Fuchs and M.E. Cates, *Phys. Rev. Lett.* **88** 98301-1 (2002).
- [163] A.M. Puertas, M. Fuchs and M.E. Cates, *Phys. Rev. E* **67** 31406 (2003).
- [164] G. Foffi, K.A. Dawson, S. Buldyrev, F. Sciortino, E. Zaccarelli and P. Tartaglia, *Phys. Rev. E* **65** 50802(R) (2002).
- [165] E. Zaccarelli, G. Foffi, K.A. Dawson, S.V. Buldyrev, F. Sciortino and P. Tartaglia, *Phys. Rev. E* **66** 41402 (2002).
- [166] F. Sciortino, P. Tartaglia and E. Zaccarelli, *Phys. Rev. Lett.* **91** 268301-1 (2003).
- [167] W. Götze and M. Sperl, *J. Phys.: Condens. Matter* **16** S4807 (2004).
- [168] E. Zaccarelli, G. Foffi, F. Sciortino and P. Tartaglia, *Phys. Rev. Lett.* **91** 108301-1 (2003).
- [169] W. Götze and M. Sperl, *Phys. Rev. E* **66** 11405 (2002).
- [170] E. Zaccarelli, G. Foffi, K.A. Dawson, F. Sciortino and P. Tartaglia, *Phys. Rev. E* **63** 31501 (2001).
- [171] M.E. Cates, *Phys. Rev. Lett.* **89** 248304-1 (2002).
- [172] M. Fuchs and M.E. Cates, *Faraday Discuss.* **123** 267 (2003).
- [173] C.B. Holmes, M. Fuchs and M.E. Cates, *Europhys. Lett.* **63** 240 (2003).
- [174] M. Fuchs and M.E. Cates, *J. Phys.: Condens. Matter* **15** S401 (2003).
- [175] A.M. Puertas, E. Zaccarelli and F. Sciortino, *J. Phys.: Condens. Matter* **17** L271 (2005).
- [176] G. Naegele and J. Bergenholtz, *J. Chem. Phys.* **108** 9893 (1998).
- [177] A.M. Puertas, M. Fuchs and M.E. Cates, *J. Chem. Phys.* **121** 2813 (2004).
- [178] A.M. Puertas, M. Fuchs and M.E. Cates, *J. Phys. Chem. B* **109** 6666 (2005).
- [179] J. Bergenholtz, W.C.K. Poon and M. Fuchs, *Langmuir* **19** 4493 (2003).
- [180] S.A. Shah, Y.-L. Chen, S. Ramakrishnan, K.S. Schweizer and C.F. Zukowski, *J. Phys.: Condens. Matter* **15** 4751 (2003).
- [181] K.G. Soga, J.R. Melrose and R.C. Ball, *J. Chem. Phys.* **108** 6026 (1998).
- [182] J.F.M. Lodge and D.M. Heyes, *Phys. Chem. Chem. Phys.* **1** 2119 (1999).
- [183] E. Zaccarelli, F. Sciortino, S.V. Buldyrev and P. Tartaglia, in *Unifying Concepts in Granular Media and Glasses*, edited by A. Coniglio, A. Fierro, H.J. Herrmann, M. Nicodemi (Elsevier, Amsterdam, 2004), p. 181.
- [184] G. Foffi, C. De Michele, F. Sciortino and P. Tartaglia, *Phys. Rev. Lett.* **94** 078301-1 (2005).
- [185] G. Foffi, C. De Michele, F. Sciortino and P. Tartaglia, *cond-mat* **0505289** (2005).
- [186] F. Sciortino, S.V. Buldyrev, C. De Michele, G. Foffi, N. Ghofraniha, E. La Nave, A. Moreno, S. Mossa, I. Saika-Voivod, P. Tartaglia and E. Zaccarelli, *Comput. Phys. Comm.* **169** 166 (2005).
- [187] G.A. Vliegenthart and P. van der Schoot, *Europhys. Lett.* **62** 600 (2003).
- [188] E. Zaccarelli, H. Löwen, P.P.F. Wessels, F. Sciortino, P. Tartaglia and C.N. Likos, *Phys. Rev. Lett.* **92** 225703-1 (2004).
- [189] J.B. Hayter and J. Penfold, *Mol. Phys.* **42** 109 (1981).

- [190] L. Belloni, *J. Phys.: Condens. Matter* **14** 9323 (2002).
- [191] H. Löwen, P.A. Madden and J.-P. Hansen, *Phys. Rev. Lett.* **68** 1081 (1992).
- [192] Y. Brumer and D.R. Reichman, *Phys. Rev. E* **69** 041202-1 (2004).
- [193] J. Dobnikar, M. Brunner, H.-H. von Gruenberg and C. Bechinger, *Phys. Rev. E* **69** 031402-1 (2004).
- [194] A.R. Denton, *J. Phys.: Condens. Matter* **11** 10061 (1999).
- [195] H.M. Lindsay and P.M. Chaikin, *J. Chem. Phys.* **76** 3774 (1982).
- [196] E.P. Wigner, *Phys. Rev.* **46** 1002 (1934).
- [197] E.P. Wigner, *Trans. Faraday Soc.* **34** 678 (1938).
- [198] E.B. Sirota, H.D. Ou-Yang, S.K. Sinha and P.M. Chaikin, *Phys. Rev. Lett.* **62** 1524 (1989).
- [199] D. Hone, S. Alexander, P.M. Chaikin and P. Pincus, *J. Chem. Phys.* **79** 1474 (1983).
- [200] S. Alexander, P.M. Chaikin, P. Grant, G.J. Morales, P. Pincus and D. Hone, *J. Chem. Phys.* **80** 5776 (1984).
- [201] W.H. Shih and D. Stroud, *J. Chem. Phys.* **79** 6254 (1983).
- [202] R.O. Rosenberg and D. Thirumalai, *Phys. Rev. A* **36** 5690 (1987).
- [203] P. Salgi and R. Rajagopalan, *Langmuir* **7** 1383 (1991).
- [204] S. Sengupta and A.K. Sood, *Phys. Rev. A* **44** 1233 (1991).
- [205] N. Choudhury and S.K. Ghosh, *Phys. Rev. E* **51** 4503 (1995).
- [206] K. Kremer, M.O. Robbins and G.S. Grest, *Phys. Rev. Lett.* **57** 2694 (1986).
- [207] M.O. Robbins, K. Kremer and G.S. Grest, *J. Chem. Phys.* **88** 3286 (1988).
- [208] E.J. Meijer and D. Frenkel, *J. Chem. Phys.* **94** 2269 (1991).
- [209] F. Sciortino, S. Mossa, E. Zaccarelli and P. Tartaglia, *Phys. Rev. Lett.* **93** 055701 (2004).
- [210] S.K. Lai, W.J. Ma, W. van Meegen and I.K. Snook, *Phys. Rev. E* **56** 766 (1997).
- [211] S.K. Lai and G.F. Wang, *Phys. Rev. E* **58** 3072 (1998).
- [212] W. Härtl, H. Versmold and X.Z. Heider, *J. Chem. Phys.* **102** 6613 (1995).
- [213] Ch. Beck, W. Härtl and R. Hempelmann, *J. Chem. Phys.* **111** 8209 (1999).
- [214] D. Bonn, H. Tanaka, G. Wegdam, H. Kellay and J. Meunier, *Europhys. Lett.* **45** 52 (1998).
- [215] P. Mongondry, J.F. Tassin and T. Nicolai, *J. Coll. Int. Sci.* **283** 397 (2005).
- [216] D. Bonn, S. Tomase, B. Abou, H. Tanaka and J. Meunier, *Phys. Rev. Lett.* **89** 015701 (2002).
- [217] H. Tanaka, J. Meunier and D. Bonn, *Phys. Rev. E* **69** 031404 (2004).
- [218] H. Tanaka, S.J. Farouji, J. Meunier and D. Bonn, *Phys. Rev. E* **71** 021402 (2005).
- [219] B. Ruzicka, L. Zulian and G. Ruocco, *Phys. Rev. Lett.* **93** 258301 (2004).
- [220] T. Nicolai and S. Cocard, *Langmuir* **16** 8189 (2000).
- [221] T. Nicolai and S. Cocard, *Eur. Phys. J. E* **5** 221 (2001).
- [222] M. Dijkstra, J.P. Hansen and P.A. Madden, *Phys. Rev. Lett.* **75** 2236 (1995).
- [223] S. Kutter, J.-P. Hansen and M. Sprik, *J. Chem. Phys.* **112** 311 (2000).
- [224] G. Odriozola, M. Romero-Bastida and F. de J. Guevara-Rodriguez, *Phys. Rev. E* **70** 021405-1 (2004).
- [225] E.J.W. Verwey and J.Th.G. Overbeek, in *Theory of the Stability of Lyophobic Colloids* (Elsevier, Amsterdam, 1948).
- [226] P.N. Segrè, V. Prasad, A.B. Schofield and D.A. Weitz, *Phys. Rev. Lett.* **86** 6042 (2001).
- [227] A.D. Dinsmore and D.A. Weitz, *J. Phys.: Condens. Matter* **14** 7581 (2002).
- [228] J. Grönwold and W.K. Kegel, *J. Phys. Chem. B* **105** 11702 (2001).
- [229] J. Grönwold and W.K. Kegel, *J. Phys.: Condens. Matter* **16** S4877 (2004).
- [230] H. Sedgwick, S.U. Egelhaaf and W.C.K. Poon, *J. Phys.: Condens. Matter* **16** S4913 (2004).
- [231] G.A. Vliegthart, J.F.M. Lodge and H.N.W. Lekkerkerker, *Phys. A* **263** 378 (1999).
- [232] A. Coniglio, L. De Arcangelis, E. Del Gado, A. Fierro and N. Sator, *J. Phys.: Condens. Matter* **16** S4831 (2004).
- [233] A. Stradner, H. Sedgwick, F. Cardinaux, W.C.K. Poon, S.U. Egelhaaf and P. Schurtenberger, *Nature* **432** 492 (2004).
- [234] P. Baglioni, E. Fratini, B. Lonetti and S.H. Chen, *J. Phys.: Condens. Matter* **16** S5003 (2004).

- [235] J. Wu, Y. Liu, W.-R. Chen, J. Cao and S.-H. Chen, *Phys. Rev. E* **70** 050401-1 (2004).
- [236] S. Mossa, F. Sciortino, P. Tartaglia and E. Zaccarelli, *Langmuir* **20** 10756 (2004).
- [237] J.D. Bernal, *Proc. Royal Soc. (London)* **280** 299 (1964).
- [238] F. Sciortino, P. Tartaglia and E. Zaccarelli, *cond-mat* **0505453** (2005).
- [239] A.I. Campbell, V.J. Anderson, J.S. van Duijneveld and P. Bartlett, *Phys. Rev. Lett.* **94** 208301-1 (2005).
- [240] H.J. Woo, C. Carraro and D. Chandler, *Phys. Rev. E* **52** 6497 (1995).
- [241] T. Ohta and K. Kawasaki, *Macromolecules* **19** 2621 (1993).
- [242] C. Sagui and R.C. Desai, *Phys. Rev. Lett.* **71** 3995 (1993).
- [243] R. Sear, S.W. Chung, G. Markovich, W.M. Gelbart and J.R. Heath, *Phys. Rev. E* **59** R6255 (1999).
- [244] A. Imperio and L. Reatto, *J. Phys.: Condens. Matter* **16** S3769 (2004).
- [245] Y. Levin and J.J. Arenzon, *J. Phys. A* **36** 5857 (2003).
- [246] F. Bordini, C. Cametti, M. Diociaiuti, D. Gaudino, T. Gili and S. Sennato, *Langmuir* **20** 5214 (2004).
- [247] F. Bordini, C. Cametti, M. Diociaiuti and S. Sennato, *Phys. Rev. E* **71** 050401-1 (2005).
- [248] C.N. Likos, H. Löwen, M. Watzlawek, B. Abbas, O. Jucknischke, J. Allgaier and D. Richter, *Phys. Rev. Lett.* **80** 4450 (1998).
- [249] D. Vlassopoulos, G. Fytas, T. Pakula and J. Roovers, *J. Phys.: Condens. Matter* **13** R855 (2001).
- [250] M. Kapnistos, D. Vlassopoulos, G. Fytas, K. Mortensen, G. Fleischer and J. Roovers, *Phys. Rev. Lett.* **85** 4072 (2000).
- [251] B. Loppinet, E. Stiakakis, D. Vlassopoulos, G. Fytas and J. Roovers, *Macromolecules* **34** 8216 (2001).
- [252] J. Stellbrink, J. Allgaler, M. Monkenbusch, D. Richter, A. Lang, C.N. Likos, M. Watzlawek, H. Löwen, G. Ehlers and P. Schleger, *Progr. Colloid Polym. Sci.* **115** 88 (2000).
- [253] E. Stiakakis, D. Vlassopoulos, C.N. Likos, J. Roovers and G. Meier, *Phys. Rev. Lett.* **89** 208302-1 (2002).
- [254] E. Stiakakis, D. Vlassopoulos, B. Loppinet, J. Roovers and G. Meier, *Phys. Rev. E* **66** 051804 (2002).
- [255] T.A. Witten and P.A. Pincus, *Macromolecules* **19** 2509 (1986).
- [256] A. Jusufi, M. Watzlawek and H. Löwen, *Macromolecules* **32** 4470 (1999).
- [257] S.K. Lai, J.L. Wang and G.F. Wang, *J. Chem. Phys.* **110** 7433 (1999).
- [258] G.F. Wang and S.K. Lai, *Phys. Rev. Lett.* **82** 3645 (1999).
- [259] C. Mayer, C.N. Likos and H. Löwen, *Phys. Rev. E* **70** 041402 (2004).
- [260] G.A. McConnell, A.P. Gast, J.S. Huang and S.D. Smith, *Phys. Rev. Lett.* **71** 2102 (1993).
- [261] T.P. Lodge, J. Bang, M.J. Park and K. Char, *Phys. Rev. Lett.* **92** 145501-1 (2004).
- [262] M. Laurati, J. Stellbrink, R. Lund, L. Willner, D. Richter and E. Zaccarelli, *Phys. Rev. Lett.* **94** 195504-1 (2005).
- [263] E.R. Weeks, *Curr. Opin. Colloid Interface Sci.* **7** 196 (2002).
- [264] J.C. Crocker and D.G. Grier, *Phys. Rev. Lett.* **73** 352 (1994).
- [265] V.N. Manoharan, M.T. Elsesser and D.J. Pine, *Science* **301** 483 (2003).
- [266] A. Yethiraj and A. van Blaaderen, *Nature* **421** 513 (2003).
- [267] E. Zaccarelli, S.V. Buldyrev, E. La Nave, A.J. Moreno, I. Saika-Voivod, F. Sciortino and P. Tartaglia, *Phys. Rev. Lett.* **94** 218301-1 (2005).